KERNFORSCHUNGSANLAGE JÜLICH GmbH
Institut für Plasmaphysik
Association EURATOM-KFA

Two-Zone Model for the Transport of Wall Released Impurities in the Edge Plasma of a Limiter Tokamak

by
Hans-Arno Claaßen
Hartmut Gerhauser

Jül-2115
February 1987
ISSN 0366-0885

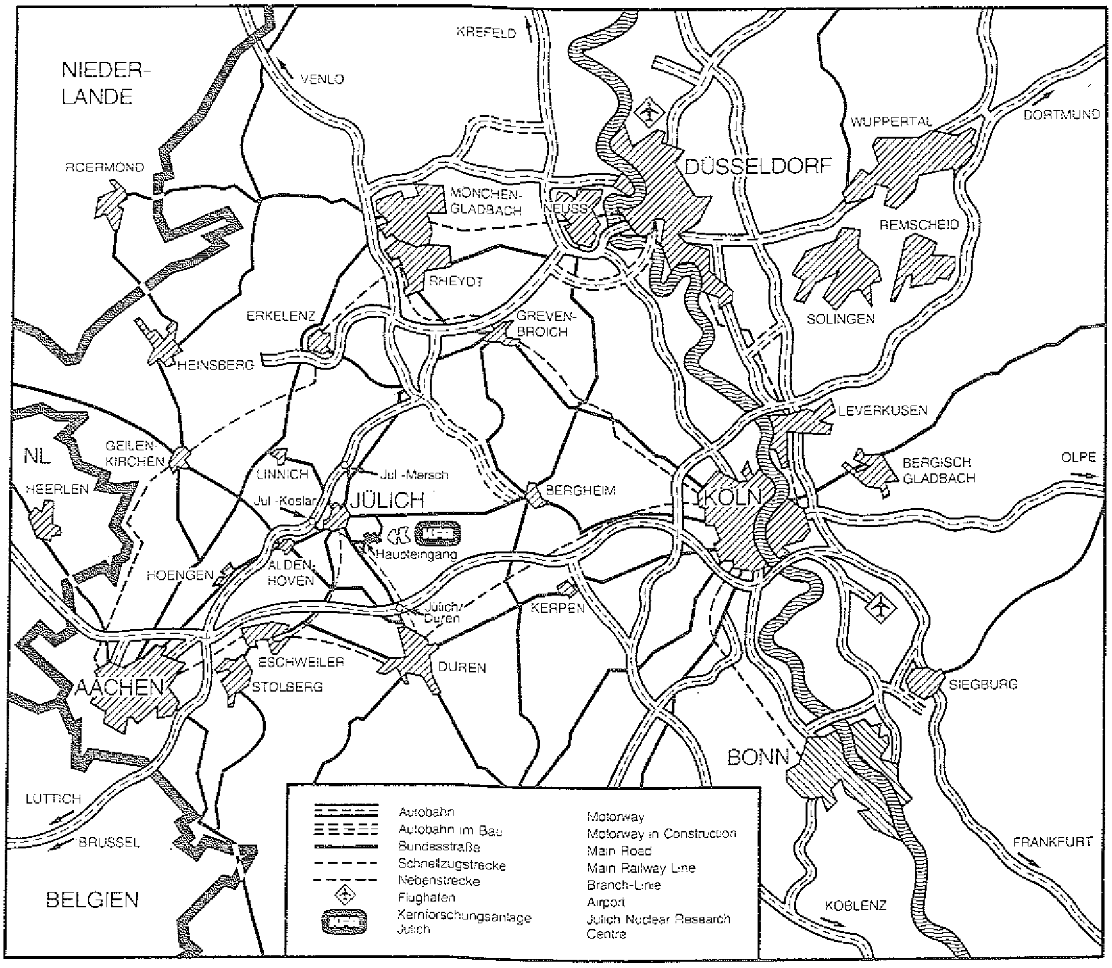

Als Manuskript gedruckt

Berichte der Kernforschungsanlagen Jülich - Nr. 2115

Institut für Plasmaphysik, Association EURATOM-KFA Jül-2115

Zu beziehen durch: ZENTRALBIBLIOTHEK der Kernforschungsanlage Jülich GmbH
Postfach 1913 · D-5170 Jülich (Bundesrepublik Deutschland)
Telefon: 02461/610 · Telex: 833556-0 kf d

Two-Zone Model for the Transport of wall released Impurities in the Edge Plasma of a Limiter Tokamak

by
Hans-Arno Claaßen
Hartmut Gerhauser

I. Introduction

In two previous papers [1,2] some aspects of the impurity transport problem in the edge region of a tokamak plasma have been theoretically investigated under consideration of both parallel-field (toroidal) convection and cross-field (radial) convection and diffusion. It was shown that under certain restrictions concerning the thermalization between impurity and hydrogen ions an analytical solution of the drift-kinetic equation for the impurity ions can be constructed by a combination of the methods of characteristics and Laplace transforms, if the plasma background is assumed to be radially homogeneous. In order to simulate the strong radial variations, which the plasma parameters undergo in the edge region, a subdivision of the plasma background into several radially homogeneous zones discontinuously connected with each other has been devised. Within each plasma zone the impurity ion population is, of course, determined by both the transport processes as well as the volume and surface sources. The latter appear in the form of particle fluxes from the limiter and from or into the adjacent plasma zones.

In order to obtain a uniform smooth solution of the impurity transport problem for the whole plasma region, the solutions for adjacent plasma zones have to be adjusted by requiring for each charge state continuity of both particle density and cross-field flux at the common boundary. If applied to the final solution, the matching procedure leads to an integral equation for either the particle density or the cross-field flux. One way of solving these integral equations is to incorporate the matching procedure directly in the Laplace transformed version of the drift-kinetic equation and to manage the additional complications in the inverse Laplace transformation. The success of this procedure depends on the choice of an appropriate variable for the Laplace transform, which should either be common to all plasma zones or subject to a simple transformation when going from one plasma zone to another. Unfortunately, the convection time, which was used in the Laplace transform in connection with the method of characteristics [1,2], does in general not fulfil the requirements of the above mentioned matching procedure.

Thus the problems encountered in the evaluation of the cross-field surface fluxes are not yet solved for the recycling of limiter released impurities or for the transmission of a toroidally <u>localized</u> impurity injection pulse.

The above mentioned mathematical difficulties disappear, however, for the transmission of a toroidally <u>uniform</u> impurity injection pulse, in which case the guiding-centre distribution functions of the various impurity ion species can be expanded into fast converging series of eigenfunctions of a combined convection-collision operator (see ref. [3]). This procedure automatically accounts for both friction and thermalization with the hydrogen ions of the background plasma. It relates the distribution function to a reference frame moving with a velocity, which in the limit $v_C \rightarrow \infty$ approaches the flow velocity of the hydrogen ions. The iterative solution applied to the transport equations for the expansion coefficients does not resort to the method of characteristics and thus avoids the difficulties encountered with the individual convection times. Instead the real time t (or the square of the diffusion length $\sqrt{D_\perp t}$, if the cross-field diffusion coefficient $D_\perp$ is constant) can be used for the Laplace transform in all plasma zones.

In the following the transmission of a Gaussian metal impurity pulse uniformly injected from the torus wall is studied within a two-zone plasma model, which separates the plasma into scrape-off layer and plasma core and allows for discontinuous changes of the plasma parameters at the separatrix. The plasma parameters are supposed to ensure a collision dominated scrape-off plasma, in which case we may restrict the solution of the transport equations to its zero order approximation.

II. <u>The model</u>

The two-zone plasma model already introduced in ref. [1] is depicted in <u>fig. 1</u> and demonstrates the way in which the radial profiles of the plasma parameters are simulated by step functions the steps being located at the separatrix. The scrape-off layer is characterized by a toroidal plasma flow and a toroidal electrostatic field, which are assumed to increase linearly towards the limiter. The impurities, which are injected uniformly from the torus wall into the plasma, are ionized by electron impact and, if ionized inside the s.o.l., are swept along the magnetic field lines due to the combined effect of electrostatic acceleration and friction with hydrogen ions flowing to the limiter. Superimposed to this parallel convection there are anomalous cross-field diffusion and convection processes due to correlations between density and poloidal electric field fluctuations. Since the parallel forces, which entrain the impurity ions along the magnetic field, are assumed to drop to zero when going to the plasma core, steep density gradients arise at the separatrix, which cause the impurity ions produced in the edge region of the plasma core to diffuse outwards into the scrape-off layer. In the time-dependent problem of the injection pulse under consideration the density profiles are smeared out in the course of time decaying to zero due to the impurity ion losses at the limiter, the torus wall and deep inside the plasma core.

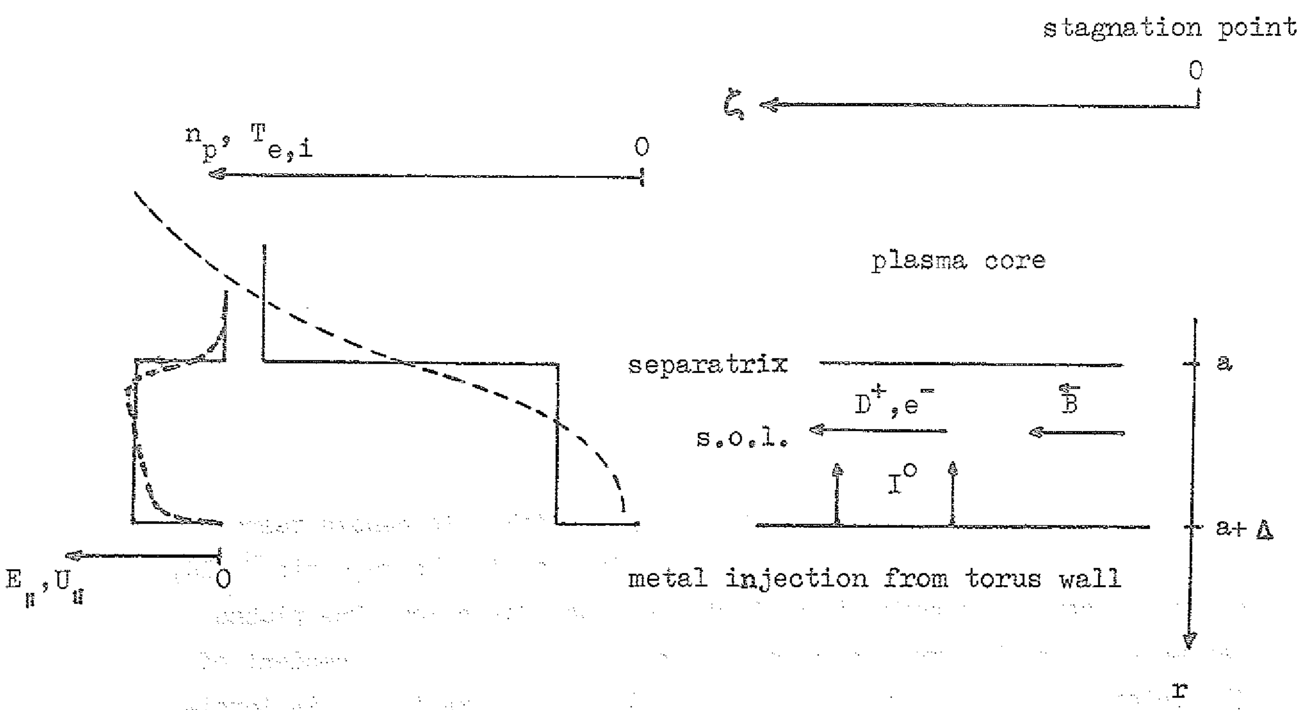

fig.1 : 'two-zone' plasma model in slab geometry
(---- actual plasma profiles, —— model)
depicted qualitatively

III. The governing equations[+]

The basis of the following study is the drift-kinetic equation for the various ionization states of a specified impurity element

Coulomb collisions with hydrogen ions
+ electrostatic acceleration $\parallel \vec{B}$

convection $\parallel \vec{B}$

$$-\frac{\partial a}{\partial t} + \frac{\partial}{\partial r}\left(D_\perp \frac{\partial a}{\partial r} - V_\perp a \right) - v_\parallel \frac{\partial a}{\partial \zeta} + Q(\vec{x}, v_\parallel, t) - \nu_I a + C_\parallel(a) = 0 \qquad (1)$$

diffusion and convection $\perp \vec{B}$

sources and ionization losses

time variations due to volume and surface sources
varying slowly on the fluctuation time-scale

Eq.(1) is averaged over $v_\perp$ and written for a slab geometry using the independent variables t, $\vec{x}=(r,\zeta)$ and $v_\parallel$. It links the space-time evolution of the ($v_\perp$-averaged) guiding-centre distribution function of the impurity ions[++]

$$a(\vec{x}, v_\parallel, t) = \frac{m_z}{kT_R} \int_0^{+\infty} dv_\perp v_\perp \bar{f}(\vec{x}, v_\parallel, v_\perp, t) \qquad (2)$$

T_R = constant reference temperature

with the background of the wall-released impurity neutrals and the hydrogen plasma through the averaged source function

---

[+] In what follows the indices $\parallel$ and $\perp$ are taken to denote respectively the directions parallel and perpendicular to the magnetic field, which is assumed to coincide with the toroidal direction. The plasma parameters and the impurity sources are supposed to be independent of the poloidal angle varying only in radial (r) and eventually in toroidal (ζ) direction. The indices e,i,o,z refer in the usual way to electrons, hydrogen ions, impurity neutrals and impurity ions of charge Ze.

[++] In eqs.(2,3) the bar indicates an average over the gyro-angle of the ion motion

$$Q(\vec{x},v_{\parallel},t) = \frac{m_z}{kT_R}\int_0^{+\infty} dv_{\perp} v_{\perp} \bar{Q}(\vec{x},v_{\parallel},v_{\perp},t) = \begin{cases} Q_N(\vec{x},v_{\parallel},t) & z=1 \\ & \text{for} \\ \nu_I a(\vec{x},v_{\parallel},t)\Big|_{z-1} & z\geq 2 \end{cases} \qquad (3)$$

and the effective collision operator (including the impurity ion acceleration in the parallel electric field $E_{\parallel}$)

$$C_{\parallel} = \nu_C\left(\underbrace{v_{Tz}^2\frac{\partial^2}{\partial v_{\parallel}^2}}_{\text{diffusion}} + \underbrace{(\alpha v_{\parallel} - \beta_{eff}v_{Tz})\frac{\partial}{\partial v_{\parallel}} + \alpha}_{\text{friction in } v_{\parallel}-\text{ space}^{+}}\right) \text{with} \begin{cases} v_{Tz} = \sqrt{\dfrac{2kT_z}{m_z}} \\ \beta_{eff} = \beta + \dfrac{ZeE_{\parallel}}{m_z v_{Tz}\nu_C} \end{cases} \qquad (4)$$

In the above equations ν_I is the electron impact ionization frequency. It is implicitly assumed that the translational state of the impurity ions does not change by electron impact ionization. ν_C, α, β denote respectively the collision frequency and collision coefficients for Coulomb collisions between impurity and hydrogen ions (see Appendix A). Note that the expressions for the macroscopic impurity ion parameters contain neither T_R nor T_z, which therefore remain undefined.

In order to solve eq.(1) we start with the ansatz (according to the method outlined in ref.[3])

$$\begin{pmatrix} a(\vec{x},v_{\parallel},t) \\ \\ Q(\vec{x},v_{\parallel},t) \end{pmatrix} = \sum_{m=0}^{\infty} \begin{pmatrix} A_m(\vec{x},t) \\ \\ Q_m(\vec{x},t) \end{pmatrix} H_m(\xi)\exp(-\xi^2) \qquad (5)$$

$^+$ By inserting the effective collision operator, eq.(4), into the defining equations for friction force as well as heating and diffusion rate in $v_{\parallel}$ - space we get

$$\begin{pmatrix} F \\ H \\ \mathcal{D} \end{pmatrix}_{\parallel z} = \frac{m_z}{2}\int_{-\infty}^{+\infty} dv_{\parallel} \begin{pmatrix} 2v_{\parallel} \\ v_{\parallel}^2 \\ (v_{\parallel}-\hat{v}_{\parallel})^2 \end{pmatrix} C_{\parallel}(a) = m_z n_z \nu_C \begin{pmatrix} \beta_{eff}v_{Tz} - \alpha\hat{v}_{\parallel} \\ v_{Tz}^2 - \alpha\widehat{v_{\parallel}^2} + \beta_{eff}v_{Tz}\hat{v}_{\parallel} \\ v_{Tz}^2 - \alpha\widehat{v_{\parallel}^2} + \alpha\hat{v}_{\parallel}^2 \end{pmatrix}$$

and therefore $H_{\parallel z} = \mathcal{D}_{\parallel z} + \hat{v}_{\parallel}F_{\parallel z}$. The symbol $\hat{A}(v_{\parallel})$ is used to denote averaging of $A(v_{\parallel})$ over the distribution function $a(\vec{x},v_{\parallel},t)$. In case of a monoenergetic impurity ion beam injected with a velocity $\hat{v}_{\parallel}$ into the hydrogen plasma we write $a(\vec{x},v_{\parallel},t) = C(\vec{x},t)\,\delta(v_{\parallel}-\hat{v}_{\parallel})$ and obtain $\mathcal{D}_{\parallel Z} = m_z n_z \nu_C v_{Tz}^2$, which is related to the second derivative with respect to $v_{\parallel}$ in eq.(4).

where $H_m(\xi)$ is a Hermite polynomial of order m in the normalized velocity

$$\xi = \sqrt{\frac{\alpha}{2}}\left(\frac{\kappa_z}{v_{T_z}} v_{\parallel} - \frac{\beta_{eff}}{\alpha\kappa_z}\right) \quad \text{with} \quad \begin{cases} 2\kappa_z^2 = 1 + \sqrt{1 + \dfrac{4}{\alpha\nu_C\tau_{\parallel}^o}} \\ \dfrac{1}{\tau_{\parallel}^o} = \dfrac{v_{Tz}}{\sqrt{\alpha}}\dfrac{\partial}{\partial\xi}\left(\dfrac{\beta_{eff}}{\sqrt{\alpha}}\right) \end{cases} \tag{6}$$

The guiding-centre distribution and the source function of the impurity ions are thus related to a reference frame moving with the velocity $\beta_{eff} v_{Tz}/\alpha\kappa_z^2$.

Eq.(5) describes a series expansion with respect to eigenfunctions of a combined convection-collision operator

$$\left(-v_{\parallel}\frac{\partial}{\partial\xi} + (C_{\parallel} + \lambda_m\nu_C)\right) H_m(\xi)\exp(-\xi^2) = 0 \tag{7}$$

with the eigenvalues

$\lambda_m = \alpha\left(\kappa_z^2(m+1) - 1\right)$ to satisfy the boundary condition

$$\lim_{v_{\parallel}\to\pm\infty} a(\vec{x}, v_{\parallel}, t) = 0 \tag{8}$$

By insertion of the series expansions for $a(\vec{x}, v_{\parallel}, t)$ and $Q(\vec{x}, v_{\parallel}, t)$ into eq.(1) we obtain the following set of transport equations for the expansion coefficients

$$\frac{\partial A_m}{\partial t} + \frac{\partial}{\partial r}\left(V_{\perp}A_m - D_{\perp}\frac{\partial A_m}{\partial r}\right) + \frac{v_{Tz}\beta_{eff}}{\alpha\kappa_z^2}\frac{\partial A_m}{\partial\xi} + (\nu_I + \lambda_m\nu_C)A_m = \tag{9}$$

$$= Q_m - \frac{v_{Tz}}{\kappa_z\sqrt{2\alpha}}\left(2(m+1)\frac{\partial A_{m+1}}{\partial\xi} + (1-\delta_{mo})\frac{\partial A_{m-1}}{\partial\xi}\right)$$

where due to the orthogonality relation for the Hermite polynomials

$$\begin{bmatrix} A_m(\vec{x},t) \\ Q_m(\vec{x},t) \end{bmatrix} = \frac{1}{2^m m!\sqrt{\pi}}\int_{-\infty}^{+\infty} d\xi \begin{bmatrix} a(\vec{x},v_{\parallel},t) \\ Q(\vec{x},v_{\parallel},t) \end{bmatrix} H_m(\xi) \tag{10}$$

The solution of eq.(9) is considerably facilitated, if we assume that the source function is uniform in toroidal direction, i.e. $\partial Q/\partial \zeta = 0$ holds, and the effective toroidal friction force increases linearly towards the limiter such that $\beta_{eff} = \beta^{*}\zeta$ (see Appendix A). In this case (by using the summation theorem for Hermite polynomials, p.1035 of ref.[7]) the expansion coefficients of the source function read

$$Q_m(\varrho,\zeta,t) = \sum_{k=0}^{m} \binom{m}{k} \frac{(-1)^k}{\sqrt{2}^{\,3m}\, m!\sqrt{2\pi}}\, H_k\!\left(\frac{\beta^{*}\zeta}{\kappa_z\sqrt{\alpha}}\right) \int_{-\infty}^{+\infty} d\xi' Q(\varrho,\xi',t) H_{m-k}(\xi')$$

$$\xi' = v_{\parallel} \frac{\kappa_z\sqrt{\alpha}}{v_{Tz}} \tag{11}$$

with the additional simplification that for a source function, which is symmetrical with respect to $v_{\parallel}$, the relation

$$\int_{-\infty}^{+\infty} d\xi' Q(\varrho,\xi',t) H_{m-k}(\xi') = 0 \quad \text{holds for odd values of } (m-k)^{+} \tag{12}$$

As is well known from transport theory each member (m) of the set of eqs.(9) is coupled with the next higher member (m+1). The system is usually closed by truncation at a specified value m=M expressing the higher moments by a combination of the lower ones. In contrast to this truncation scheme we decouple the set of eqs.(9) completely in zero order approximation neglecting the moments A_{m+1} in the eq. for A_m. The latter are introduced successively in higher approximations. It can be shown (see ref.[3]) that the successive approximations converge for a toroidally uniform source distribution and that the convergence improves with increasing value of the parameter $(\nu_I + \lambda_m \nu_C)\kappa_z^2 \tau_{\parallel}^{o} \geq 1$.

+ As a particular application of this relation we obtain from eq.(11)

$$Q_1(\varrho,\zeta,t) = -\frac{\beta^{*}\zeta}{\kappa_z\sqrt{2\alpha}} Q_o(\varrho,t)$$

In zero order approximation, which is already close to the exact solution in the collision dominated case, the transport equations for m=0 and m=1 reduce to

$$-\frac{\partial A_m^o}{\partial t} + \frac{\partial}{\partial r}\left(D_\perp \frac{\partial A_m^o}{\partial r} - V_\perp A_m^o\right) - \left(\nu_I + \lambda_m \nu_C + \frac{\delta_{m1}}{\kappa_z^2 \tau_\parallel^o}\right) A_m^o = - Q_m^o \qquad (13)$$

where
$$\lambda_o \nu_C = \frac{1}{\kappa_z^2 \tau_\parallel^o} = \frac{\beta^* v_{Tz}}{\kappa_z^2 \alpha} \qquad (14)$$

In the limit $\nu_C \rightarrow \infty$ $(\kappa_z^2 \rightarrow 1)$ the fluxes in the moving reference frame disappear so that $A_1^o \rightarrow 0$ and $\Gamma_\parallel^o \rightarrow (v_{Tz}\beta^*\zeta/\alpha)\, n_z^o$ for the particle flux in the laboratory reference frame. This corresponds to a shifted Maxwellian velocity distribution for $a(\vec{x}, v_\parallel, t)$ with a centre-of-mass velocity $(v_{Tz}\beta^*\zeta/\alpha)$, which is equal to the flow velocity of the hydrogen ions.

IV. The solution for a two-zone plasma

under the special assumptions
$$\begin{cases} D_\perp = \text{const.}^{+} \\ V_\perp = 0 \\ \partial Q/\partial\zeta = 0, \quad Q = Q(v_\parallel^2) \end{cases}$$

Under the above assumptions the transport equation for the coefficient $A_o^o(\varrho,t)$, which is proportional to the density distribution of the impurity ions with charge Ze, reads
$$n_z^o(\varrho,t) = \frac{1}{\kappa_z}\sqrt{\frac{2\pi k T_R}{m_z}}^{\,3} \frac{A_o^o(\varrho,t)}{\sqrt{\frac{T_R}{T_i}}}$$

$$-\frac{\partial A_o^o}{\partial \eta} + \frac{\partial^2 A_o^o}{\partial \varrho^2} - \varkappa A_o^o = -\frac{Q_o^o(\varrho,\eta)}{D_\perp} \qquad (15)$$

where $\varrho = r-a$ (a = radial position of the separatrix), $\eta = D_\perp t$ and

$$\varkappa = \begin{cases} \dfrac{\nu_I + \lambda_o \nu_C}{D_\perp} & \text{in the scrape-off layer (zone I)} \\[2ex] \dfrac{\nu_I}{D_\perp} & \text{in the plasma core (zone II)} \end{cases} \qquad (16)$$

+ In case $D_{\perp I} \neq D_{\perp II}$ different radial coordinate scalings $\varrho_R = \varrho/\sqrt{D_{\perp R}}$ must be introduced.

Using the Laplace transformation+

$$\left.\begin{aligned}\bar{a}(\varrho,p) &= \int_0^{+\infty} A_o^o(\varrho,\eta)\exp(-p\eta)\,d\eta \\ \bar{Q}(\varrho,p) &= \int_0^{+\infty} \frac{Q_o^o(\varrho,\eta)}{D_\perp}\exp(-p\eta)\,d\eta\end{aligned}\right\} \quad (17)$$

we arrive at the equation

$$\frac{d^2\bar{a}}{d\varrho^2} - (p+\varkappa)\,\bar{a} = -F(\varrho,p) \quad \text{with} \quad F(\varrho,p) = \bar{Q}(\varrho,p) + A_o^o(\varrho,0) \qquad (18)$$

If we subject this equation to the boundary conditions

$$\left.\begin{aligned}\bar{a}(-\infty,p) &= 0 \\ \bar{a}(\Delta,p) &= 0 \\ -\frac{d\bar{a}}{d\varrho}(0,p) &= \bar{\gamma}^*(p)\end{aligned}\right\} \quad (19)$$

where Δ denotes the radial position of the torus wall, from which the impurities are injected, we obtain the following solution

for $-\infty \leq \varrho \leq 0$ (plasma core, $q_{II} = \sqrt{p + \varkappa_{II}}$)

$$\bar{a}_{II}(\varrho,p) = -\int_\varrho^0 d\sigma\, F(\sigma,p)\,\frac{\sinh\left[q_{II}(\sigma-\varrho)\right]}{q_{II}} + \qquad (20a)$$

$$\cosh(q_{II}\varrho)\int_{-\infty}^0 d\sigma\, F(\sigma,p)\,\frac{\exp(q_{II}\sigma)}{q_{II}} - \bar{\gamma}^*(p)\,\frac{\exp(q_{II}\varrho)}{q_{II}}$$

+ In what follows the bar indicates Laplace transformed quantities for $0 \leq \varrho \leq \Delta$ (scrape-off layer, $q_I = \sqrt{p + \varkappa_I}$)

$$\bar{a}_I(\varrho,p) = \int_0^{\varrho} d\sigma\, F(\sigma,p)\, \frac{\sinh\left[q_I(\sigma-\varrho)\right]}{q_I} + \qquad (20b)$$

$$+ \frac{1}{\cosh(q_I\Delta)} \left(\cosh(q_I\varrho) \int_0^{\Delta} d\sigma\, F(\sigma,p)\, \frac{\sinh\left[q_I(\Delta-\sigma)\right]}{q_I} + \bar{\gamma}^*(p)\, \frac{\sinh\left[q_I(\Delta-\varrho)\right]}{q_I} \right)$$

$\bar{\gamma}^*(p)$ results from the continuity condition $\bar{a}_I(0,p) = \bar{a}_{II}(0,p)$ such that

$$\bar{\gamma}^*(p) \left(\frac{\mathrm{tgh}(q_I\Delta)}{q_I} + \frac{1}{q_{II}} \right) = \qquad (21)$$

$$= \int_{-\infty}^{0} d\sigma\, F(\sigma,p)\, \frac{\exp(q_{II}\sigma)}{q_{II}} - \frac{1}{\cosh(q_I\Delta)} \int_0^{\Delta} d\sigma\, F(\sigma,p)\, \frac{\sinh\left[q_I(\Delta-\sigma)\right]}{q_I}$$

Although this solution is amenable to the inverse Laplace transformation by using the series expansion

$$\frac{1}{1+\exp(-2q_I\Delta)} = \sum_{n=0}^{\infty} (-1)^n \exp(-2nq_I\Delta)$$

we assume in the following that $2\sqrt{\Delta^2\varkappa_I} \gg 1$, in which case the solution simplifies considerably. Then, apart from the immediate neighbourhood of the injection plane at $\varrho = \Delta$, the solution is well approximated by its limiting form for $\Delta^2\varkappa_I \rightarrow \infty$, if we leave the source function unchanged, i.e. if we suppose that $Q_o^o(\varrho,t) = 0$ for $\varrho > \Delta$.

We therefore start from this limiting form of the solution corresponding to the boundary condition $\bar{a}(+\infty,p) = 0$ (deviations caused by the boundary condition $\bar{a}(\Delta,p) = 0$ are shown in the limit $\exp(-2\sqrt{\Delta^2\varkappa_I}) \ll 1$ for one example) to perform the inverse Laplace transformation (see Appendix B). By use of the abbreviations

$\varkappa^* = \varkappa_I - \varkappa_{II}$, I_1 = modified Bessel function of first order

$$Q^o_{oR}(\sigma,t-\tau') = \left(Q_o^o(\sigma,t-\tau') + 2A_o^o(\sigma,0)\,\delta(t-\tau')\right)\exp(-\varkappa_R D_\perp \tau') \qquad \text{for} \quad R=I,II$$

the solution can be written in the following form (after being transformed back into real time):

for $\underline{-\infty \le \varrho \le 0}$ (plasma core)

$$A_o^o(\varrho,t) = \int_{-\infty}^{0} d\sigma \int_0^t d\tau' \, \frac{Q^o_{oII}(\sigma,t-\tau')}{2\sqrt{\pi D_\perp}} \left[\frac{\exp\left(-\frac{(\varrho-\sigma)^2}{4D_\perp\tau'}\right)}{\sqrt{\tau'}} - \int_0^{\tau'} \frac{d\tau}{\tau} \, \frac{\exp\left(-\frac{(\varrho+\sigma)^2}{4D_\perp(\tau'-\tau)} - \varkappa^* D_\perp \frac{\tau}{2}\right)}{\sqrt{\tau'-\tau}} \, I_1\!\left(\varkappa^* D_\perp \frac{\tau}{2}\right) \right] +$$

for $\underline{\varrho = 0}$

$$\exp(-\varkappa^* D_\perp \tau') \int_0^{\tau'} d\tau \, \frac{\exp(\varkappa^* D_\perp \tau)-1}{\sqrt{\tau(\tau'-\tau)}^{\,3}} \, \sigma \exp\left(-\frac{\sigma^2}{4D_\perp(\tau'-\tau)}\right) \qquad (22a)$$

$$\int_0^{\Delta} d\sigma \int_0^t d\tau' \, \frac{Q^o_{oII}(\sigma,t-\tau')}{4\pi\varkappa^* D_\perp^2}$$

for $\underline{-\infty \le \varrho < 0}$

$$\left[\int_0^{\tau'} d\tau \, \frac{\exp\left(-\varkappa^* D_\perp\tau - \frac{\varrho^2}{4D_\perp(\tau'-\tau)} - \frac{\sigma^2}{4D_\perp\tau}\right)}{\sqrt{\tau(\tau'-\tau)}^{\,3}} \left(\varrho + \sigma - \frac{\varrho\sigma}{2D_\perp}\left(\frac{\varrho}{\tau'-\tau} + \frac{\sigma}{\tau}\right)\right) - \frac{\varrho \exp\left(-\frac{\varrho^2}{4D_\perp\tau'}\right)}{\frac{\sqrt{\tau'}^{\,3}}{4\sqrt{\pi D_\perp}}} \, \delta(\sigma) \right]$$

for $\underline{0 \leq \varrho \leq \Delta}$ (scrape-off layer)

$$A_o^o(\varrho,t) = \int_0^\Delta d\sigma \int_0^t d\tau' \frac{Q_{oI}^o(\sigma,t-\tau')}{2\sqrt{\pi D_\perp}} \left[\frac{\exp\left(-\frac{(\varrho-\sigma)^2}{4D_\perp\tau'}\right)}{\sqrt{\tau'}} + \int_0^{\tau'} \frac{d\tau}{\tau} \frac{\exp\left(-\frac{(\varrho+\sigma)^2}{4D_\perp(\tau'-\tau)} + \varkappa^* D_\perp \frac{\tau}{2}\right)}{\sqrt{\tau'-\tau}} I_1\left(\varkappa^* D_\perp \frac{\tau}{2}\right) \right] +$$

$$\text{for } \underline{\varrho = 0} \longrightarrow \exp(\varkappa^* D_\perp \tau') \int_0^{\tau'} d\tau \frac{\exp(-\varkappa^* D_\perp \tau) - 1}{\sqrt{\tau(\tau'-\tau)}^3} \, \sigma \exp\left(-\frac{\sigma^2}{4D_\perp(\tau'-\tau)}\right) \tag{22b}$$

$$+ \int_{-\infty}^0 d\sigma \int_0^t d\tau' \frac{Q_{oI}^o(\sigma,t-\tau')}{4\pi\varkappa^* D_\perp^2}$$

$$\text{for } \underline{0 < \varrho \leq \Delta} \longrightarrow \left[\int_0^{\tau'} d\tau \frac{\exp\left(\varkappa^* D_\perp \tau - \frac{\varrho^2}{4D_\perp(\tau'-\tau)} - \frac{\sigma^2}{4D_\perp \tau}\right)}{\sqrt{\tau(\tau'-\tau)}^3} \left(\varrho + \sigma - \frac{\varrho\sigma}{2D_\perp}\left(\frac{\varrho}{\tau'-\tau} + \frac{\sigma}{\tau}\right)\right) - \frac{\varrho \exp\left(-\frac{\varrho^2}{4D_\perp\tau'}\right)}{\frac{\sqrt{\tau'}^3}{4\sqrt{\pi D_\perp}}} \delta(\sigma) \right]$$

It can be shown that eq.(22a) fits continuously to eq.(22b) at $\varrho = 0$ (see Appendix C) and that in the limit $\varkappa_I = \varkappa_{II} = \varkappa$, i.e. for a completely homogeneous plasma background, a unified solution of the form

$$A_o^o(\varrho,t) = \int_{-\infty}^\Delta d\sigma \int_0^t d\tau' \left(Q_o^o(\sigma,t-\tau') + 2A_o^o(\sigma,0)\,\delta(t-\tau')\right) \frac{\exp\left(-\varkappa D_\perp \tau' - \frac{(\varrho-\sigma)^2}{4D_\perp \tau'}\right)}{2\sqrt{\pi D_\perp \tau'}} \tag{23}$$

results from eqs.(22a,b) by use of $I_1(0) = 0$ and application of l'Hospital's rule.

Going to the limit $\Delta^2 \varkappa_I \to \infty$ we obtain the following solution of eq.(21)
(see Appendix D)

$$- D_\perp \frac{\partial A_o^o(\varrho,t)}{\partial \varrho}\bigg|_{\varrho=0} = - \int_{-\infty}^{0} d\sigma \int_0^t d\tau' \, \frac{\sigma \, Q_{oII}^o(\sigma, t-\tau')}{4\sqrt{\pi D_\perp}} \left[\frac{\exp\left(-\frac{\sigma^2}{4D_\perp \tau'}\right)}{\sqrt{\tau'}^3} + \int_0^{\tau'} \frac{d\tau}{\tau} \frac{\exp\left(-\frac{\sigma^2}{4D_\perp(\tau'-\tau)} - \overset{*}{\varkappa} D_\perp \frac{\tau}{2}\right)}{\sqrt{\tau'-\tau}^3} I_1\left(\overset{*}{\varkappa} D_\perp \frac{\tau}{2}\right) \right]$$

$$- \int_0^{\Delta} d\sigma \int_0^t d\tau' \, \frac{\sigma \, Q_{oI}^o(\sigma, t-\tau')}{4\sqrt{\pi D_\perp}} \left[\frac{\exp\left(-\frac{\sigma^2}{4D_\perp \tau'}\right)}{\sqrt{\tau'}^3} - \int_0^{\tau'} \frac{d\tau}{\tau} \frac{\exp\left(-\frac{\sigma^2}{4D_\perp(\tau'-\tau)} + \overset{*}{\varkappa} D_\perp \frac{\tau}{2}\right)}{\sqrt{\tau'-\tau}^3} I_1\left(\overset{*}{\varkappa} D_\perp \frac{\tau}{2}\right) \right] \qquad (24)$$

V. The source function $Q_o(\sigma, t-\tau')_{z=1}$

Under sole consideration of electron impact ionization (neglecting recombination processes) we get for the source function of singly ionized impurities

$$Q_N(\vec{x}, v_\parallel, t) = \frac{m_z \nu_o}{2\pi \, kT_R} \int_0^{2\pi} d\varphi \int_0^{+\infty} dv_\perp v_\perp f_o(\vec{x}, \vec{v}, t) \quad \text{where} \quad \begin{cases} \nu_o = \nu_{I,z=0} \\ \vec{v} = (v_\parallel, v_\perp, \varphi) \end{cases} \qquad (25)$$

In order to calculate $Q_N(\vec{x}, v_\parallel, t)$ we therefore have to solve the kinetic equation for the distribution function $f_o(\vec{x}, \vec{v}, t)$ of the injected impurity atoms

$$\frac{\partial f_o}{\partial t} - v_\perp \cos\varphi \frac{\partial f_o}{\partial \varrho} = -\nu_o f_o \tag{26}$$

φ is the inclination angle of the vector $\vec{v}_\perp$ with respect to the normal direction of the injection plane (torus wall). After electron impact ionization of the injected impurity atoms φ coincides with the initial value of the gyro-angle of the impurity ion orbit. Because of the restriction to a toroidally uniform distribution of density and temperature of the electrons and a toroidally uniform impurity injection into the scrape-off plasma f_o does not depend on ζ. For a time-dependent impurity injection at the radial position $\varrho = \Delta$ the solution of eq.(26) reads

$$f_o(\vec{x},\vec{v},t) = F_o\left(\vec{v},\ t - \frac{(\Delta-\varrho)}{v_\perp \cos\varphi},\ \Delta\right) \exp\left(-\frac{\nu_o(\Delta-\varrho)}{v_\perp \cos\varphi}\right) \tag{27}$$

If we assume a two temperature shifted Maxwellian velocity distribution

$$F_o\left(\vec{v},\ t - \frac{(\Delta-\varrho)}{v_\perp \cos\varphi},\ \Delta\right) = \frac{n_W\left(t - \frac{(\Delta-\varrho)}{v_\perp \cos\varphi}\right)}{\sqrt{\pi}^3\ v_{T_\parallel} v_{T_\perp}^2} \exp\left(-\frac{v_\parallel^2}{v_{T_\parallel}^2} - \frac{(v_\perp \sin\varphi)^2 + (v_\perp \cos\varphi - V_W)^2}{v_{T_\perp}^2}\right) \tag{28}$$

for the injected impurity atoms (V_W being the average injection velocity antiparallel to the ϱ - axis), we obtain the following expression for the first expansion coefficient (m=0) of the source function $Q_N(\vec{x}, v_\parallel, t)$ by combination of eqs.(11) and (25)

$$Q_o(\varrho,t)\Big|_{z=1} = \frac{2\nu_o K_z}{\sqrt{\frac{2\pi k T_R}{m_z}}^3} \frac{\sqrt{\frac{T_R}{T_i}}}{\pi v_{T_\perp}^2} \int_0^{+\infty} dv_\perp v_\perp \int_0^{\pi/2} d\varphi\, n_W\left(t - \frac{(\Delta-\varrho)}{v_\perp \cos\varphi}\right) \exp\left(-\frac{\nu_o(\Delta-\varrho)}{v_\perp \cos\varphi} - \frac{(v_\perp \sin\varphi)^2 + (v_\perp \cos\varphi - V_W)^2}{v_{T_\perp}^2}\right) \tag{29}$$

assuming $\alpha = \sqrt{2T_z/T_i}$ (see ref. [3]). In zero order approximation $Q_o^o(\varrho,t)_{z=1}$ is equal to the expression given in eq.(29).

In the limit $v_{T_\perp} \rightarrow 0$, which we will consider for simplicity in the numerical evaluation of eqs.(22) and (24), eq.(29) reduces to

$$\lim_{v_{T_\perp} \rightarrow 0} Q_o(\varrho,t)\Big|_{z=1} = \frac{\nu_o K_z \sqrt{\frac{T_R}{T_i}}}{\sqrt{\frac{2\pi k T_R}{m_z}}^3} n_w\left(t - \frac{\Delta-\varrho}{V_w}\right)\exp\left(-\frac{\nu_o(\Delta-\varrho)}{V_w}\right) \tag{30}$$

Assuming a Gaussian injection pulse of the form

$$n_w(t) = \frac{N_w}{V_w t_o \sqrt{\pi}} \exp\left(-\frac{(t-t_1)^2}{t_o^2}\right) \tag{31}$$

we finally end up in the formula

$$\lim_{v_{T_\perp} \rightarrow 0} Q_o^o(\sigma,t-\tau')\Big|_{z=1} = \frac{\nu_o K_z N_w \sqrt{\frac{T_R}{T_i}}}{V_w t_o \sqrt{\pi}\sqrt{\frac{2\pi k T_R}{m_z}}^3} \exp\left[-\left(\frac{t-t_1-\tau'}{t_o} - \frac{\Delta-\sigma}{V_w t_o}\right)^2 - \frac{\nu_o(\Delta-\sigma)}{V_w}\right] \tag{32}$$

Since the time-delay t_1 of the Gaussian injection pulse is at our disposal, we may always neglect the initial distribution $A_o^o(\sigma,0)$ in eqs.(22) and (24) by choosing an appropriately large value of t_1 . Note that the source function changes discontinuously at the separatrix due to the jump in the plasma parameters.

VI. Numerical results and discussion

General features of the solution (independent of the ionization level considered) can already be seen by inspection of eqs.(22 a,b) and eq.(24). It is characteristic for the problem at hand and the corresponding solution method that the impurity ion concentration (and its radial derivative) of a given charge species has to be calculated by an integral over the source points σ and different preceding times $(\tau', \tau'-\tau)$ weighted by Green's function. The latter contains the parameters $\varkappa^{*} D_{\perp}(\tau', \tau'-\tau)$ and $(\varrho, \sigma)/\sqrt{D_{\perp}(\tau', \tau'-\tau)}$, which reflect the influence of the plasma parameter jump at the separatrix and the effect of the diffusive cross-field transport on the impurity ion concentration at the point ϱ under consideration. Within the adopted model, which neglects recombination processes, the source function depends solely on the space-time distribution of the ion density in the next lower charge state. The source of the first ionization level, eq.(32), is determined by the parameters $(t-\tau-t_1)/t_o - (\Delta-\sigma)/V_w t_o$ and $\nu_o(\Delta-\sigma)/V_w$ describing the finite transit time and the attenuation by electron impact ionization of the neutral impurity beam injected from the torus wall at $\varrho = \Delta$.

By inserting eq.(32) into eqs.(22 a,b) and eq.(24) and performing the σ-integration we arrive at some lengthy expressions not given here. The parameters, which govern the space-time distribution of singly charged impurity ions, have been compiled in table 1. When going to higher ionization levels we have to perform additional three-fold integrations for each ionization step, which leads to increasingly complex expressions. In order to obtain some preliminary informations about the relation between the space-time distribution of the impurity ions and the various source and loss processes, we have (in a first computation series) postponed the time-consuming calculations for $z \geq 2$ and concentrated on $z=1$ using artificially increased convection losses in the scrape-off layer (increased by a factor of 1oo in the examples shown).

In figs.2-11 numerical results for Ti^+- ions (using the cross-sections given in ref.[4]) are plotted in the normalized form

$$\left.\frac{n_1^o(\varrho,t)}{\dfrac{N_w}{V_w t_o}}\right|_{Ti^+} \quad \text{for the density distribution and}$$

$$\left.\left(\frac{\partial n_1^o(\varrho,t)}{\dfrac{N_w}{V_w t_o}}\right) \middle/ \left(\frac{\partial \varrho}{\sqrt{\dfrac{\Delta D_\perp}{V_w}}}\right)\right|_{\varrho=0,\ Ti^+}$$

for the particle flux across the separatrix.

The results are presented for two observation times and various jump conditions for the plasma parameters at the separatrix keeping the scrape-off plasma parameters constant and assuming that the parallel friction and electric forces disappear in the plasma core.

	parameter	measures
in source function	$\left(\frac{\Delta \nu_o}{V_w}\right)_{sol}$	radial decay of the source function due to electron impact ionization
	$\left(\nu_o t_o\right)_{sol,pc}$	ionization probability within the half-life of the injection pulse
	$\frac{t-t_1-\Delta/V_w}{t_o}$	time difference to the arrival time of the injection maximum at $\varrho = 0$
	$\frac{\Delta}{V_w t_o}$	impurity transit time during the half-life of the injection pulse
in Green's function	$\frac{\Delta}{\sqrt{D_\perp t}}$	diffusive cross-field spreading of impurity ions during the time interval t
	$\left(\frac{\beta^* v_T}{\alpha \nu_o \kappa^2_{z=1}} + \frac{\nu_1}{\nu_o}\right)_{sol} ; \left(\frac{\nu_1}{\nu_o}\right)_{pc}$	losses due to parallel transport and electron impact ionization relative to the production rate
	$\left(\frac{\varkappa^* D_\perp}{\nu_o}\right)_{sol,pc}$	plasma parameter jump at the separatrix

<u>table 1</u> : characteristic parameters for z=1

t= observation time

ϱ = point under consideration

sol = scrape-off layer , pc = plasma core

As is to be expected, the (for z=1 artificially) large effect of parallel transport losses decreases drastically the particle density inside the s.o.l. and produces (in the advanced phase of the injection pulse) a negative density gradient at the separatrix with a corresponding particle flux from the plasma core into the s.o.l. (figs.2-5). Two density maxima appear: one inside the plasma core, where parallel transport losses are absent, the other inside the s.o.l.. The density profiles follow to some extent the source distribution: the density peaks near the separatrix, where the source function changes discontinuously due to the discontinuous change of the ionization frequencies, and depending on the transit time of the injected neutrals through the s.o.l. is more or less elevated near the injection plane, where the source function jumps from zero to a finite value when going from $\varrho > \Delta$ to $\varrho \leq \Delta$. An increase of the electron density and temperature jump at the separatrix leads to a shift of the (impurity) density maxima inside the plasma core towards the separatrix. This is correlated with a more pronounced peaking of the source function near the separatrix and a stronger ionization loss in the plasma core (keeping the scrape-off plasma parameters constant). One should notice that within the parameter range considered the ionization frequencies for Ti increase more slowly with the electron temperature than with the electron density and that with increasing electron temperature the differences in the ionization frequencies of the various charge states become smaller.

The magnitude and position of the density maxima are, of course, time-dependent following the injection pulse with a certain time delay. This is clearly seen from the time evolution of the particle flux across the separatrix (figs.6-7). In the case $\Delta/V_w t_o \cong 1$ (realized by the parameter combination $kT_w = 1$ eV, $t_o = 10\,\mu s$ and $\Delta = 2$ cm) the time delay is, of course, larger than for the case $\Delta/V_w t_o \ll 1$ (realized by $kT_w = 25$ eV, $t_o = 40\,\mu s$ and $\Delta = 2$ cm). The time for the maximum particle flux across the separatrix to occur shifts towards the central injection time t_1 with increasing electron density and temperature jump at the separatrix. An analysis of these data for different observation times (figs.8-11) yields a nonmonotonic variation of the cross-field particle flux with the electron temperature jump at the separatrix and a (mostly) monotonic variation with the electron density jump (within the range $1 \leq \chi n_p \leq 10$ and for observation times near t_1; an example for a later observation time is shown in fig.11).

References:

[1,2] H.A. Claaßen, H. Gerhauser: The influence of cross-field diffusion and convection on the impurity ion transport in the limiter shadow region of a tokamak, pts.I/II, KFA-reports JÜL-1971/2035 (1985)

[3] H.A. Claaßen, H. Repp: Impurity transport calculations for the limiter shadow region of a tokamak, Nucl. Fusion 21(5), 589 (1981)

[4] W. Lotz: Electron impact ionization cross-sections and ionization rate coefficients for atoms and ions from Scandium to Zinc, Garching-report IPP 1/76 (1968)

[5] G.E. Roberts, H. Kaufman: Table of Laplace transforms, W.B. Saunders Co., Philadelphia & London (1966)

[6] G.A. & Th.M. Korn: Mathematical Handbook for Scientists and Engineers, Mc Graw Hill Book Co. Inc., New York, Toronto & London (1961)

[7] I.S. Gradshteyn & I.M. Ryzhik: Table of Integrals, Series, and Products, Academic Press, New York & London (1965)

List of figures:

All figures refer to the following injection and scrape-off plasma data:

- injection rate of the Ti^o- neutrals

$$\frac{n_w(t)}{\frac{N_w}{V_w t_o}} = \frac{1}{\sqrt{\pi}} \exp\left[-\left(\frac{t-t_1}{t_o}\right)^2\right]$$

assuming $t_1 = 2t_o$ in order to ensure simultaneously $A_o^o(\varrho,0) \cong 0$ and a still acceptable computation time

- s.o.l. thickness $\Delta = 2$ cm (position of the injection plane $\varrho = \Delta$)

- scrape-off plasma parameters $\left\{ \begin{array}{l} n_p = 10^{12}/cm^3 \\ kT_e = kT_i = 10\ eV \quad , \ D_\perp = 10^4\ cm^2/s \\ U_\parallel ,\ E_\parallel \text{ according to the simple} \\ \text{1-d plasma model outlined in App. A} \end{array} \right.$

They show in detail:

→ normalized radial density profiles (in zero order approximation)

$$\left. \frac{n_1^o(\varrho, t)}{\frac{N_w}{V_w t_o}} \right|_{Ti^+}$$ at a fixed observation time t in figs.2-5

for three different jump conditions ($\chi \equiv \frac{|_{pc}}{|_{sol}}$) at the separatrix

χn_p	1	10	1
χT_e	1	1	10

keeping in mind that $\chi U_\parallel = \chi E_\parallel = 0$

fig.2, fig.3: $kT_w = 25\ eV \ , \ t_o = 40\,\mu s$ and $t = t_1 \left\{ \begin{array}{l} + \frac{t_o}{2} \\ - \frac{t_o}{2} \end{array} \right.$

fig. 4, fig.5: $kT_w = 1\ eV \ , \ t_o = 10\,\mu s$ and $t - t_o = t_1 \left\{ \begin{array}{l} + \frac{t_o}{2} \\ - \frac{t_o}{2} \end{array} \right.$

$kT_w = m_z V_w^2/2$ is the kinetic energy of the injected neutrals

fig.2 also contains the case $\varkappa^{\ddagger} = 0$ and the correction due to the boundary condition $n_1^o(\Delta, t) = 0$ as well as plots of the normalized source function

$$Q^{\ddagger}(\varrho, t) = \frac{\nu_o t_o}{\sqrt{\pi}} \frac{\Delta}{\sqrt{D_\perp t_o}} \exp\left[- \left. \frac{\nu_o \Delta}{V_w} \right|_{sol} \right] \exp\left[- \left(\frac{t - t_1}{t_o} - \frac{\Delta - \varrho}{V_w t_o} \right)^2 + \frac{\nu_o \varrho}{V_w} \right]$$

for $t = 100\,\mu s$.

$\longrightarrow$ normalized particle flux across the separatrix

$$\left.\frac{\partial\left(\dfrac{n_1^o(\varrho,t)}{\dfrac{N_w}{V_w t_o}}\right)}{\partial\left(\dfrac{\varrho}{\sqrt{\dfrac{\Delta D_\perp}{V_w}}}\right)}\right|_{\varrho=0,\ Ti^+}$$

- as a function of time within the interval $\frac{t_o}{2} \leq t \leq \frac{9t_o}{2}$ in figs.6-7

  for three different jump conditions ($\chi \equiv \frac{|pc}{|sol}$) at the separatrix

χn_p	1	10	1
χT_e	1	1	10

keeping in mind that $\chi U_\parallel = \chi E_\parallel = 0$

with $kT_w = 25$ eV , $t_o = 40\,\mu s$ in fig.6

$kT_w = 1$ eV , $t_o = 10\,\mu s$ in fig.7

- as a function of χT_e for $\chi n_p = 1$ in figs.8-9

- as a function of χn_p for $\chi T_e = 1$ in figs.10-11

  at two observation times

$$t = t_1 \pm \frac{t_o}{2} \quad \text{with } kT_w = 25 \text{ eV},\ t_o = 40\,\mu s \quad \text{in figs.8/10}$$

$$t - t_o = t_1 \pm \frac{t_o}{2} \quad \text{with } kT_w = 1 \text{ eV},\ t_o = 10\,\mu s \quad \text{in figs.9/11}$$

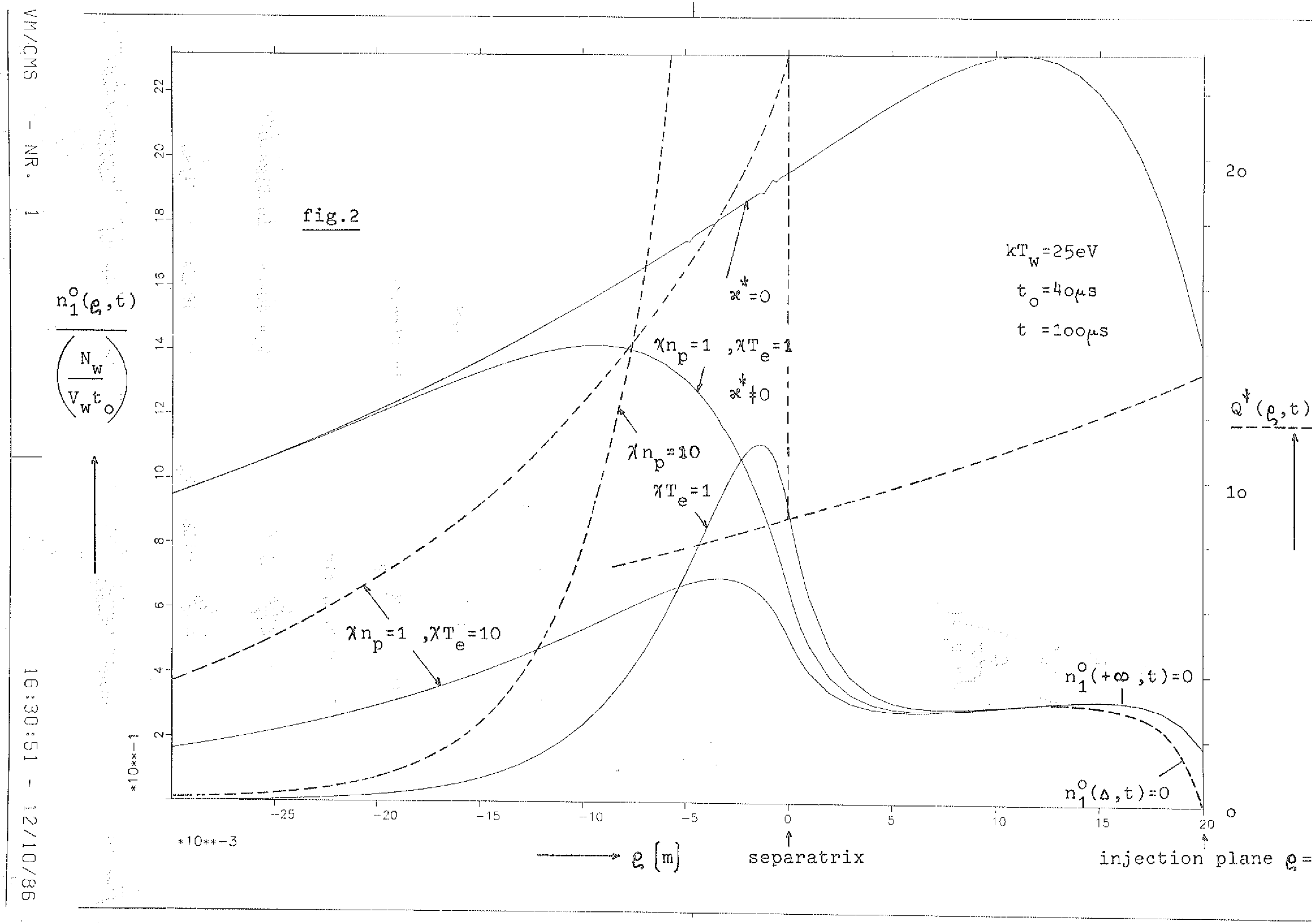
VM/CMS - NR. 1
16:30:51 - 12/10/86
$n_1^o(\varrho,t) \Big/ \left(\frac{N_w}{V_w t_o}\right)$
*10**-1
*10**-3
$\longrightarrow \varrho\,[m]$
separatrix
injection plane $\varrho = \Delta$
$Q^{\ddagger}(\varrho,t)$
kT_w=25eV
t_o=40μs
t =100μs
$\varkappa^*$=0
χn_p=1 ,χT_e=1
$\varkappa^* \neq 0$
χn_p=10
χT_e=1
χn_p=1 ,χT_e=10
$n_1^o(+\infty,t)=0$
$n_1^o(\Delta,t)=0$

fig.2

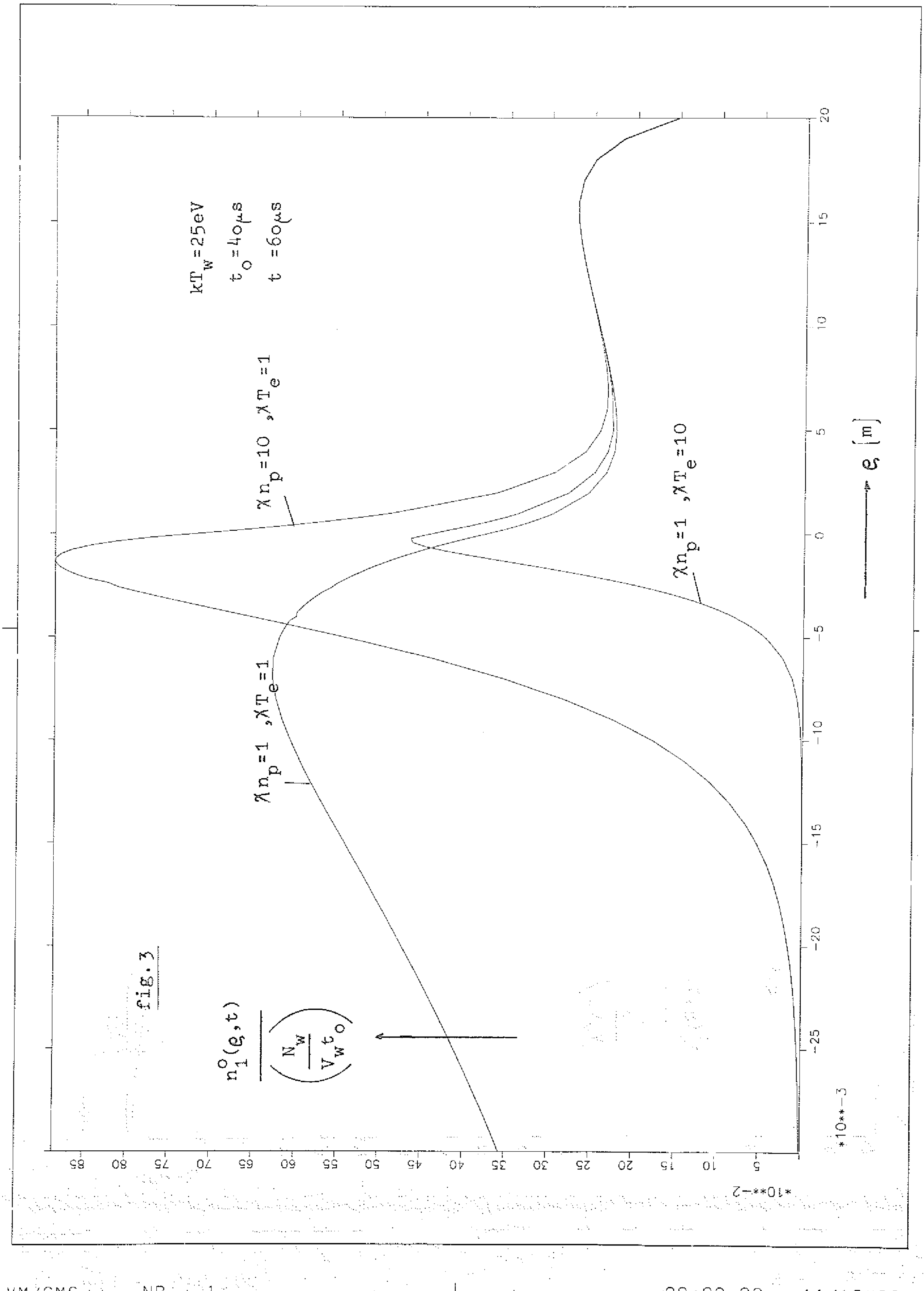
kT_W=25eV
t_o=40μs
t =60μs
χn_p=10 ,χT_e=1
χn_p=1 ,χT_e=10
χn_p=1 ,χT_e=1
ρ [m]
n_1^o(ρ,t) / (N_w / (V_w t_o))
*10**-2
*10**-3
-25 -20 -15 -10 -5 0 5 10 15 20
5 10 15 20 25 30 35 40 45 50 55 60 65 70 75 80 85

fig.3

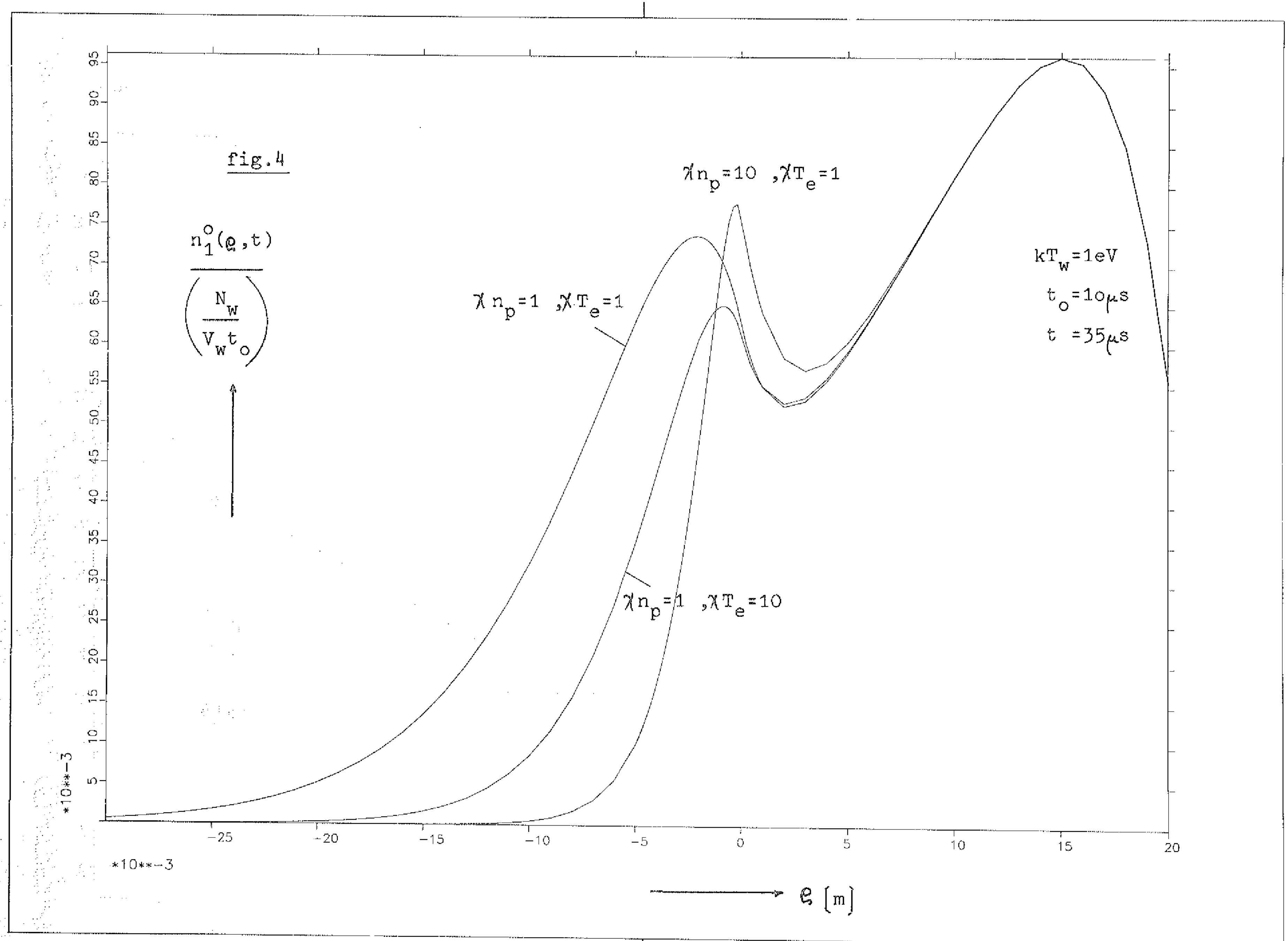

ϱ [m]
*10**-3
$n_1^o(\varrho,t) \Big/ \left(\frac{N_w}{V_w t_o}\right)$
$\chi n_p=10$,$\chi T_e=1$
$\chi n_p=1$,$\chi T_e=1$
$\chi n_p=1$,$\chi T_e=10$
$kT_w=1eV$
$t_o=10\mu s$
$t\ =35\mu s$

fig.4

-24-

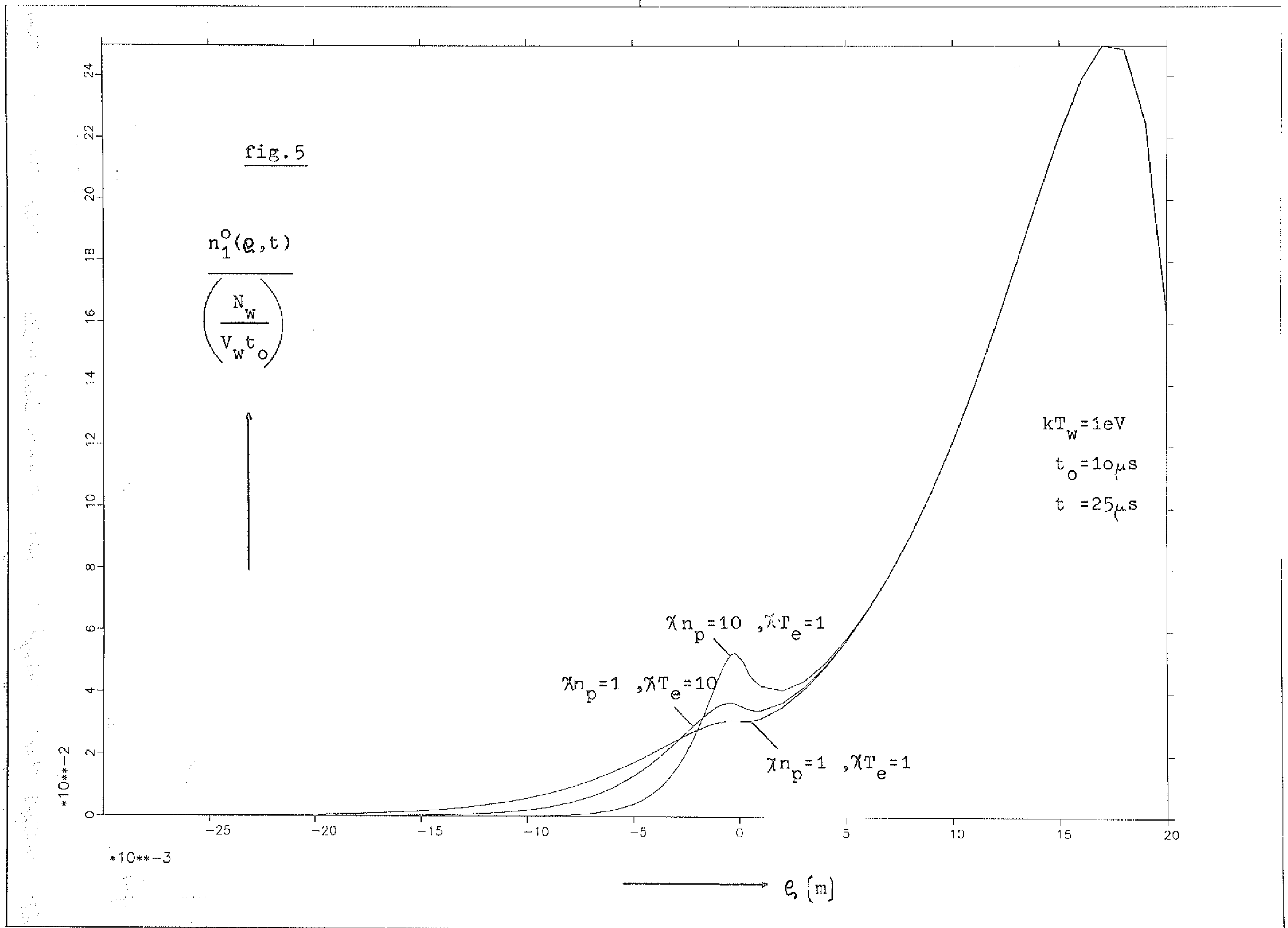
fig.5
$\dfrac{n_1^o(\varrho,t)}{\left(\dfrac{N_w}{V_w t_o}\right)}$
kT_w=1eV
t_o=10μs
t =25μs
χn_p=10 ,χT_e=1
χn_p=1 ,χT_e=10
χn_p=1 ,χT_e=1
*10**-2
*10**-3
ϱ [m]
0 2 4 6 8 10 12 14 16 18 20 22 24
-25 -20 -15 -10 -5 0 5 10 15 20

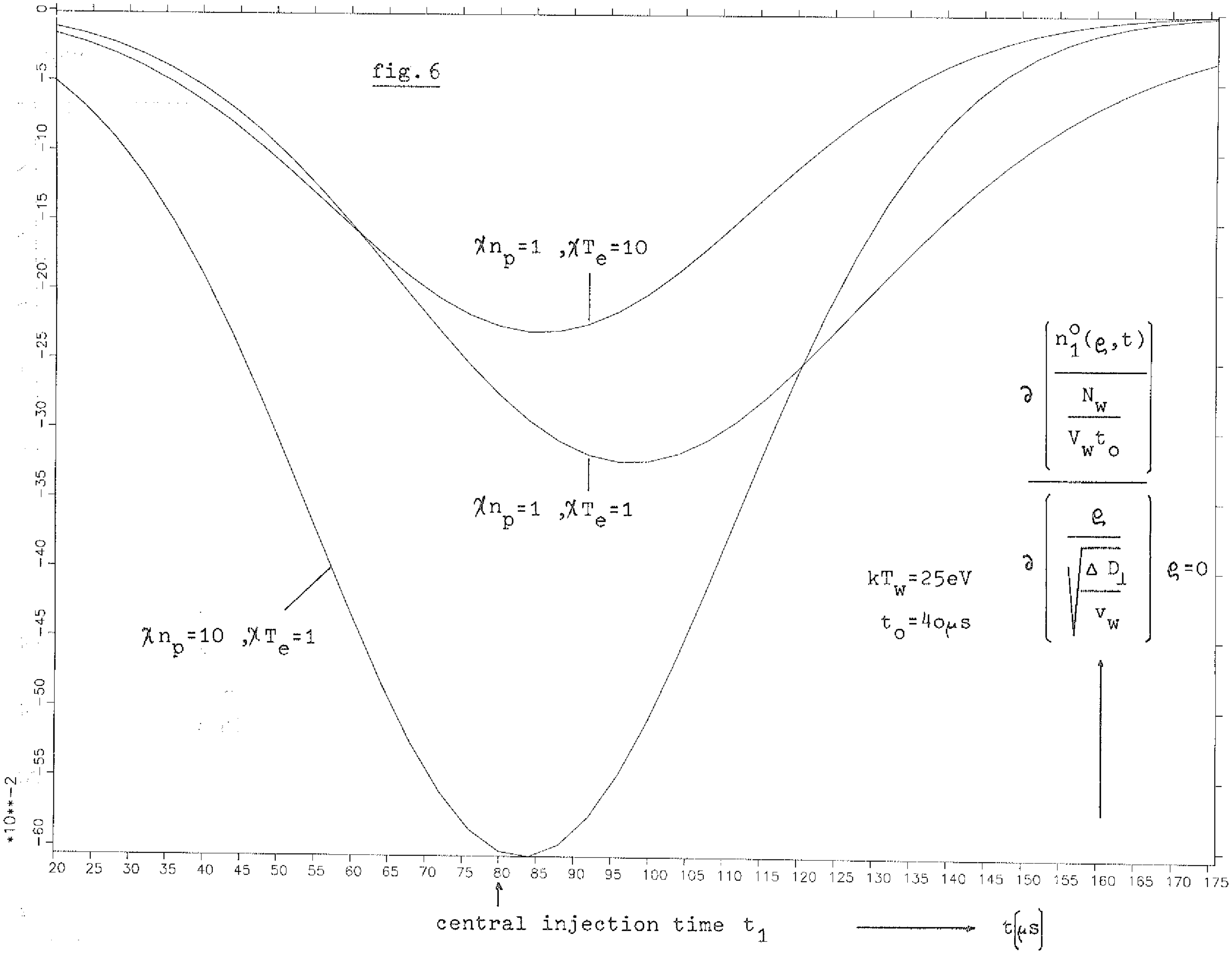
fig. 6
$\chi n_p=1$, $\chi T_e=10$
$\chi n_p=1$, $\chi T_e=1$
$\chi n_p=10$, $\chi T_e=1$
$kT_w=25eV$
$t_o=40\mu s$
$\dfrac{\partial\left(\dfrac{n_1^o(\varrho,t)}{\dfrac{N_w}{V_w t_o}}\right)}{\partial\left(\dfrac{\varrho}{\sqrt{\dfrac{\Delta D_\perp}{v_w}}}\right)}\ \varrho=0$
*10**-2
0
-5
-10
-15
-20
-25
-30
-35
-40
-45
-50
-55
-60
20 25 30 35 40 45 50 55 60 65 70 75 80 85 90 95 100 105 110 115 120 125 130 135 140 145 150 155 160 165 170 175
central injection time t_1
$t[\mu s]$

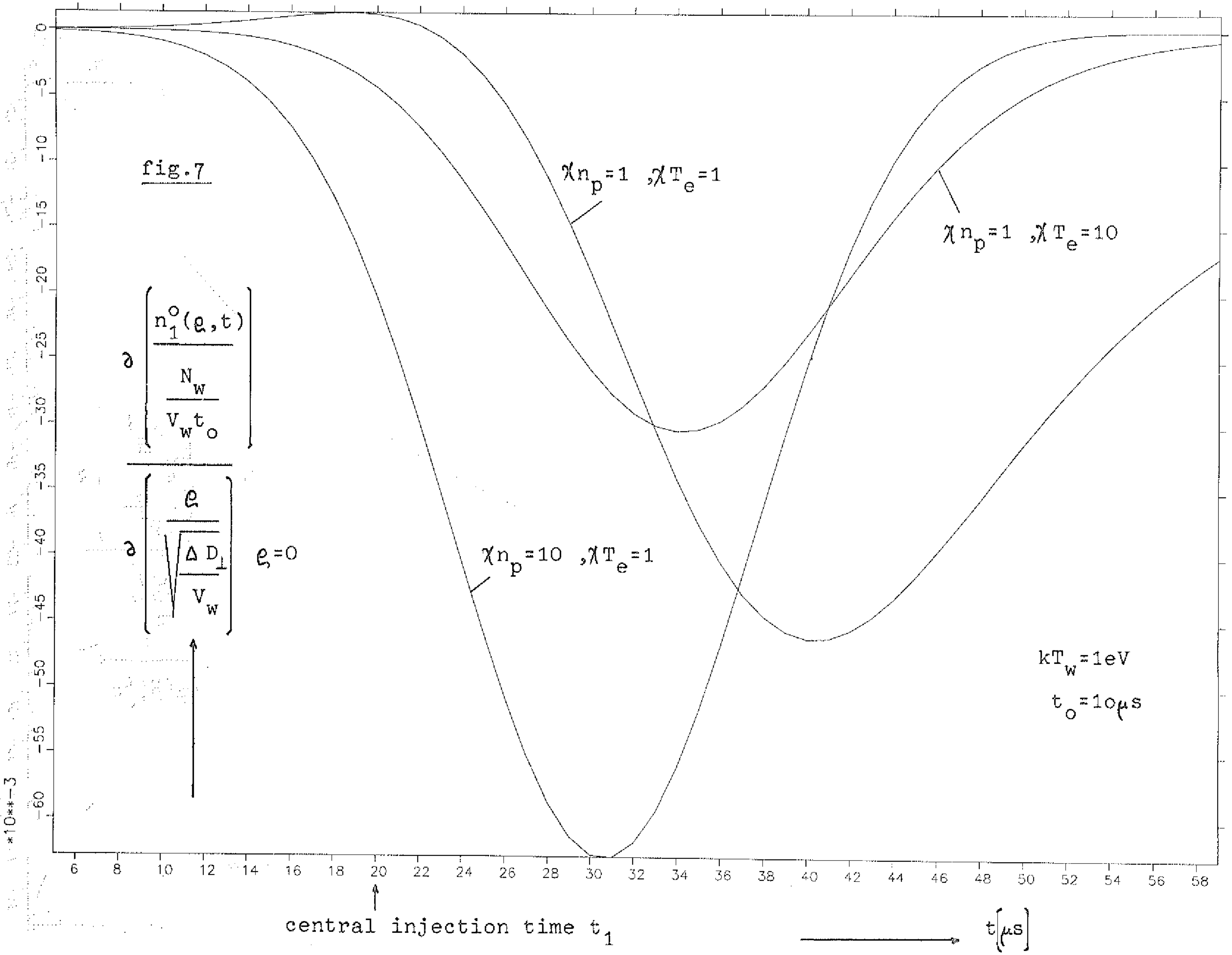

$$\frac{\partial\left[\dfrac{n_1^o(\varrho,t)}{\dfrac{N_w}{V_w t_o}}\right]}{\partial\left[\dfrac{\varrho}{\sqrt{\dfrac{\Delta D_\perp}{V_w}}}\right]}\quad \varrho=0$$

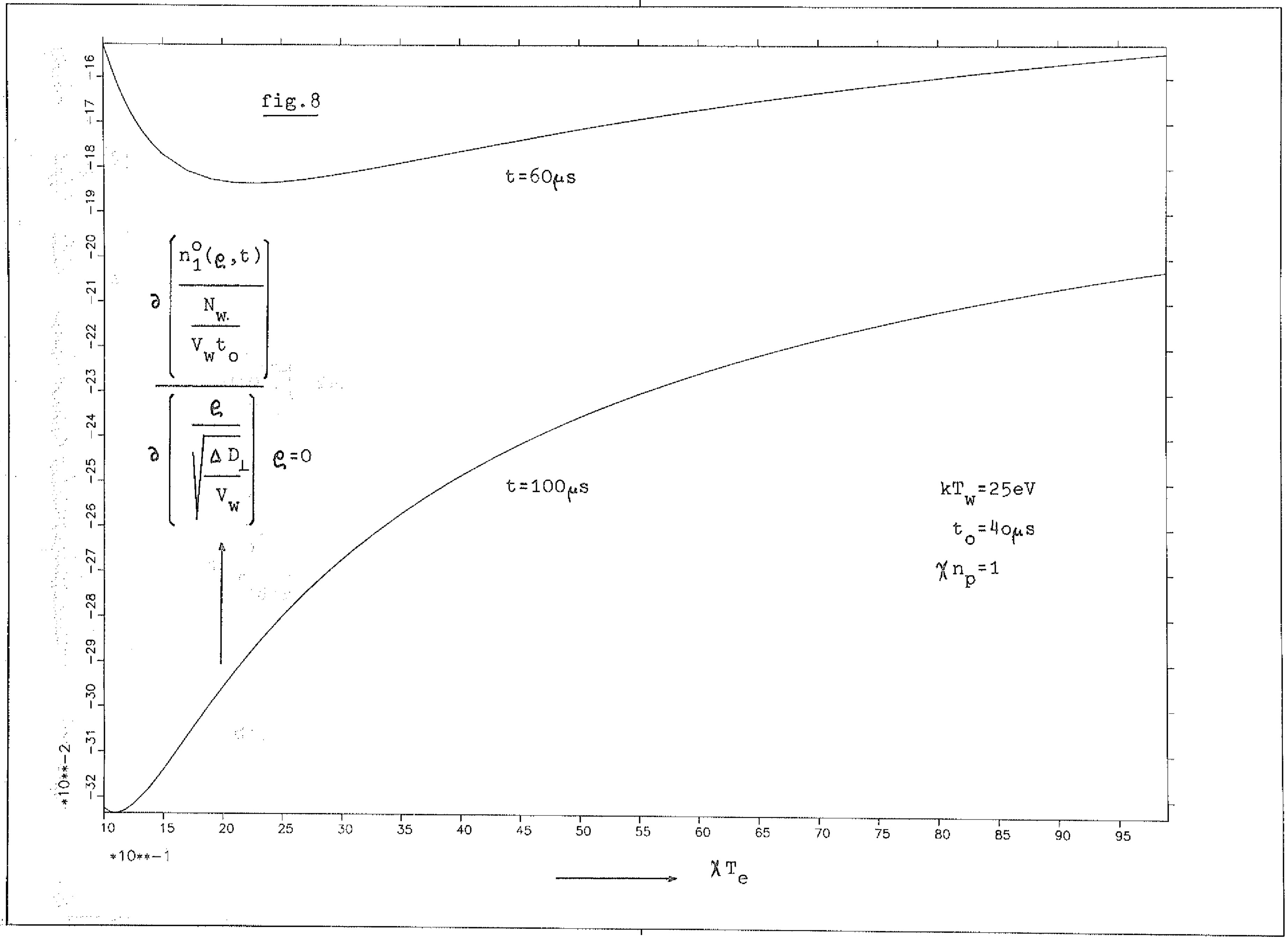

fig.8
t=60μs
t=100μs
kT_w=25eV
t_o=40μs
χn_p=1
χT_e
*10**-1
*10**-2
$\left(\frac{n_1^o(\varrho,t)}{\frac{N_w}{V_w t_o}}\right) \Bigg/ \left(\frac{\varrho}{\sqrt{\frac{\Delta D_\perp}{V_w}}}\right)$ ϱ=0

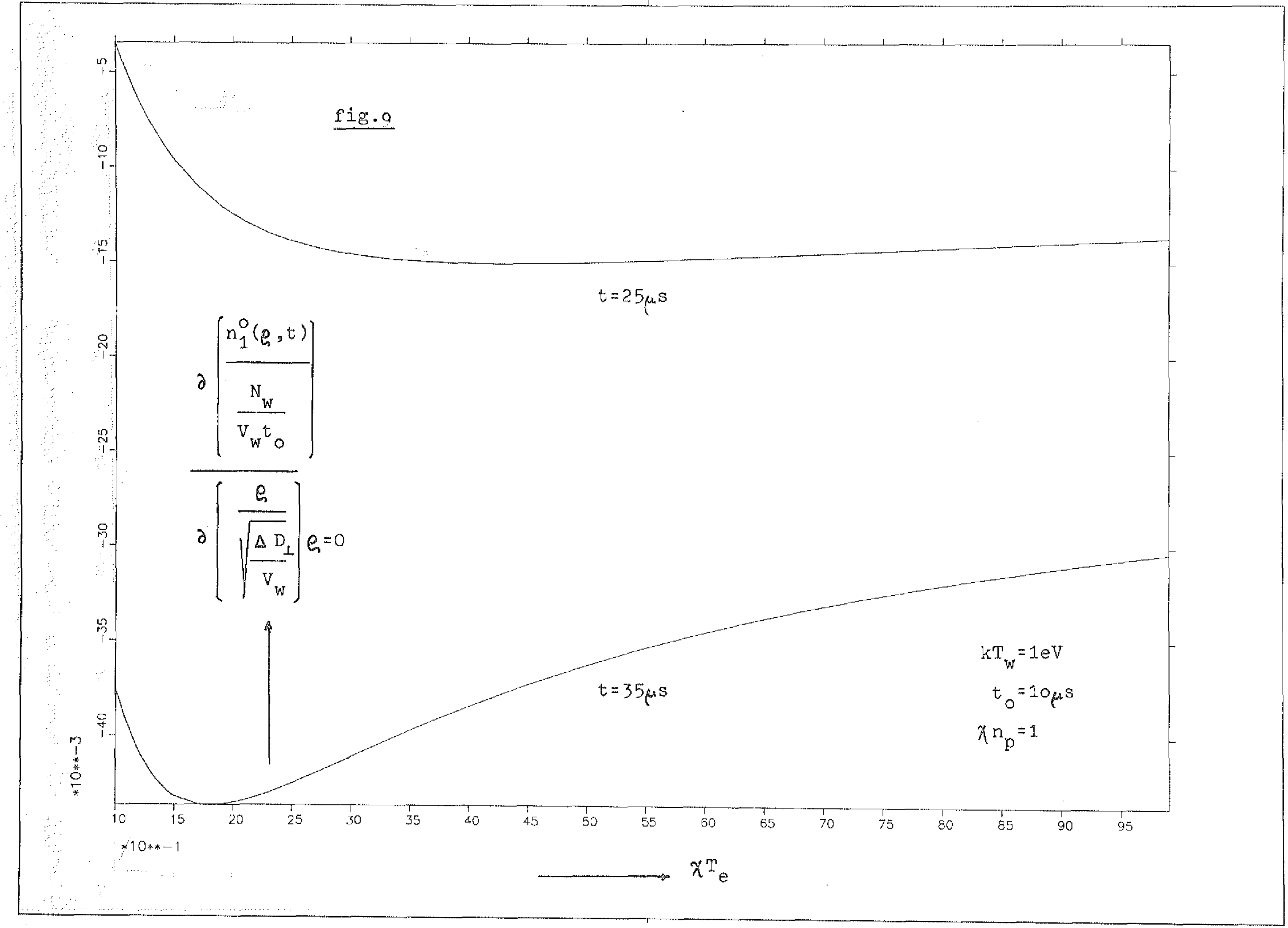

-5
-10
-15
-20
-25
-30
-35
-40
*10**-3
10
15
20
25
30
35
40
45
50
55
60
65
70
75
80
85
90
95
*10**-1
t=25μs
t=35μs
$$\frac{\partial\left[\dfrac{n_1^o(\varrho,t)}{\dfrac{N_w}{V_w t_o}}\right]}{\partial\left[\dfrac{\varrho}{\sqrt{\dfrac{\Delta D_\perp}{V_w}}}\right]}\Bigg|_{\varrho=0}$$
$kT_w=1eV$
$t_o=10\mu s$
$\chi n_p=1$
χT_e

fig.9

VM/CMS - NR. 1 14:06:19 - 12/15/86

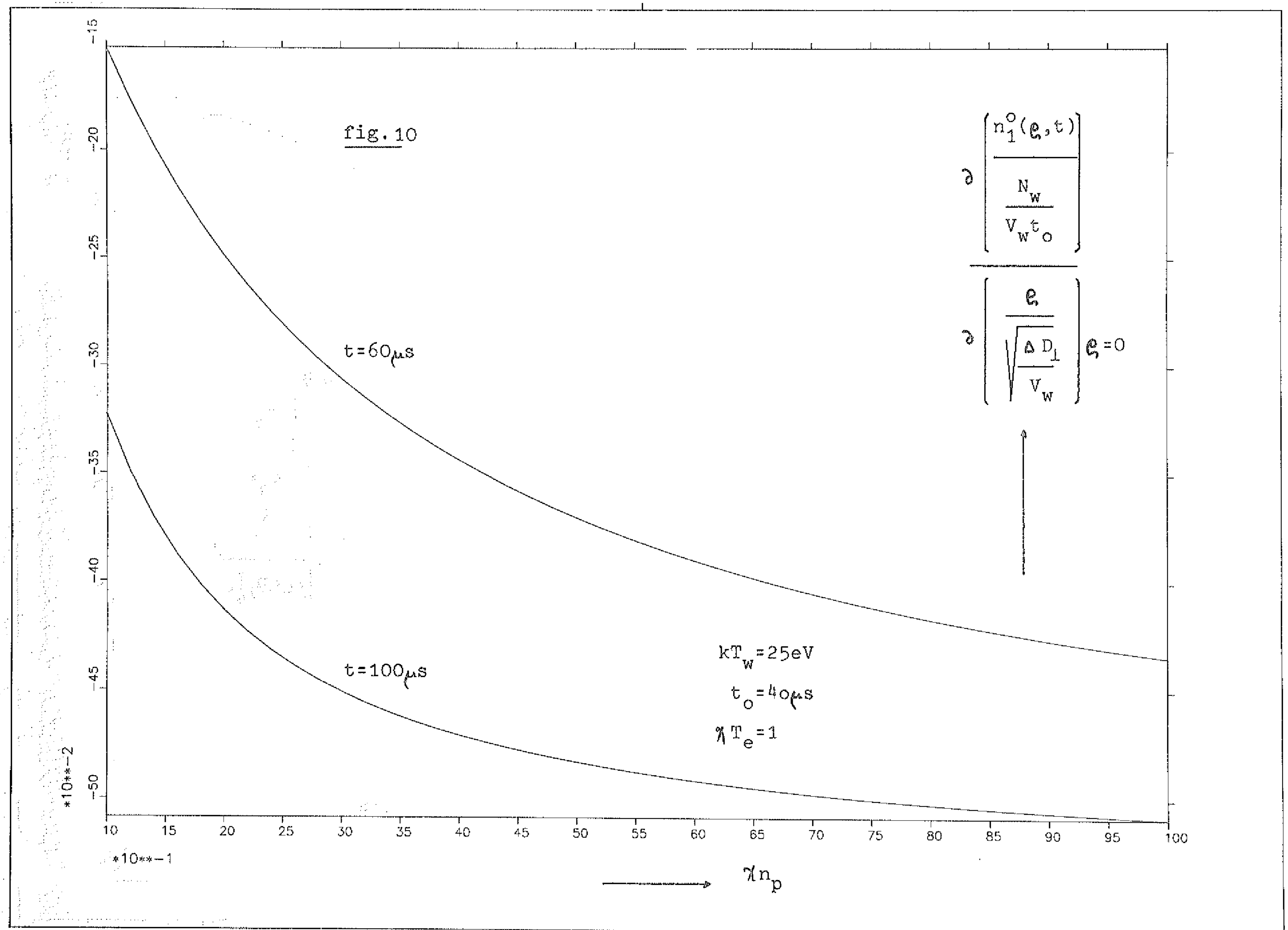

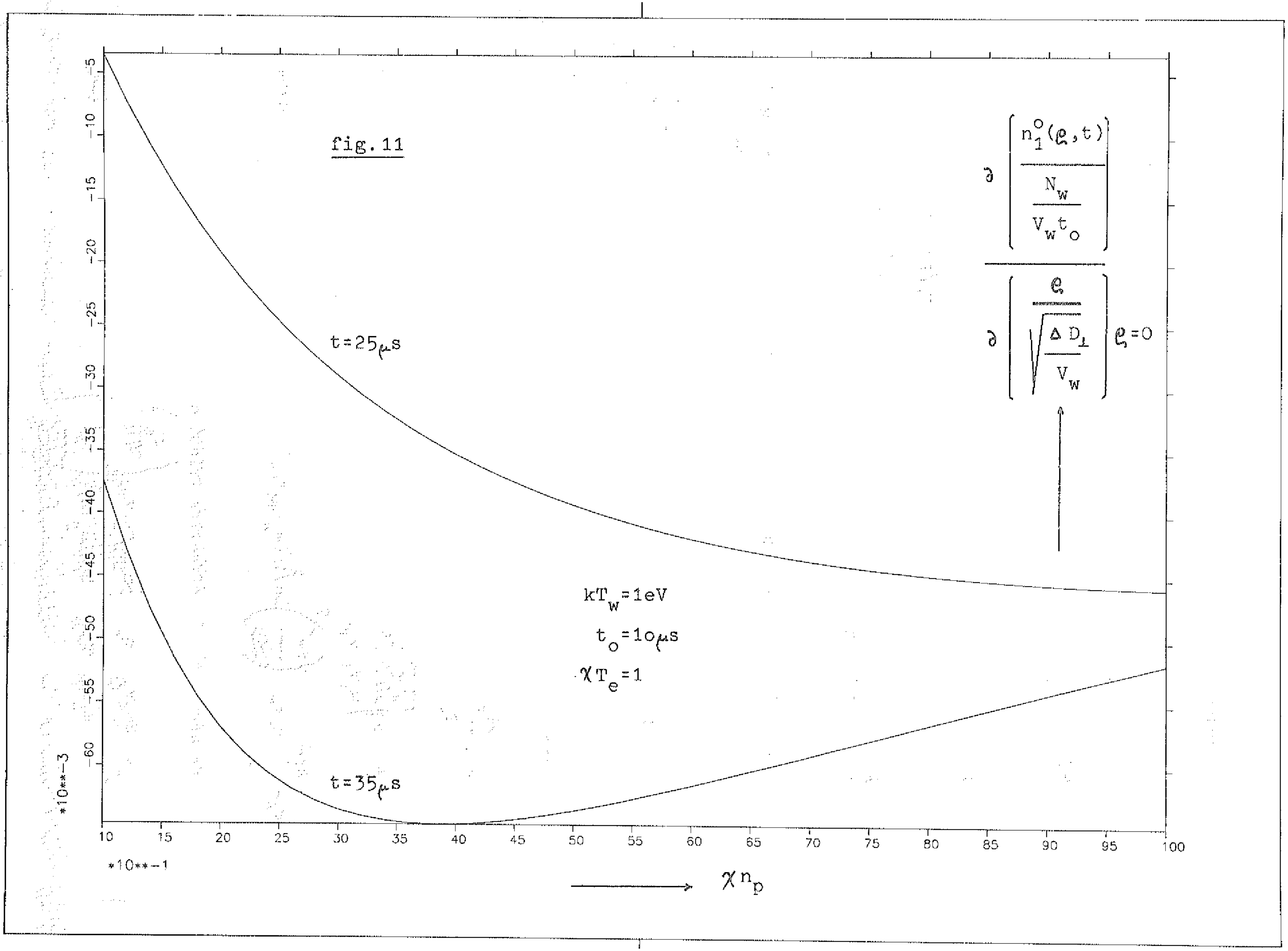

VM/CMS - NR. 1 14:05:18 - 12/15/86

Appendix A

Our simple 1-d plasma model for the scrape-off layer is based on the equations

$$\frac{\partial (n_p U_\parallel)}{\partial \zeta} = S_p$$

$$\left.\begin{aligned} &\frac{\partial p_e}{\partial \zeta} + e n_p E_\parallel = 0 \\ &\frac{\partial p_i}{\partial \zeta} - e n_p E_\parallel + m_i n_p U_\parallel \frac{\partial U_\parallel}{\partial \zeta} = - m_i U_\parallel S_p \end{aligned}\right\} \quad E_\parallel = \frac{m_i U_\parallel}{2e}\left(\frac{\partial U_\parallel}{\partial \zeta} + \frac{S_p}{n_p}\right) \tag{A1}$$

Assuming $T_e = T_i$, $(n_p, S_p) =$ const., and $U_\parallel = c_s$ for $\zeta = \pi R_o$ (c_s = ion sound velocity of the hydrogen ions in front of the limiter surface), we obtain from eq.(A1)

$$U_\parallel = \frac{c_s \zeta}{\pi R_o} \quad \text{and} \quad E_\parallel = \frac{m_i c_s^2}{e \pi R_o} \frac{\zeta}{\pi R_o} \quad \text{implying that } T_{e,i} = T^o_{e,i} - \frac{m_i c_s^2}{2}\left(\frac{\zeta}{\pi R_o}\right)^2 \tag{A2}$$

Using the collision coefficients [3]

$$\alpha = \frac{2 T_z}{T_i}$$

$$\beta = 2\sqrt{\frac{m_z T_z}{m_i T_i}}\,\frac{U_\parallel}{v_{Ti}} \tag{A3}$$

$$\nu_c = \frac{8\sqrt{\pi}}{3} n_p v_{Ti} \left(\frac{Z e^2}{4\pi\varepsilon_o}\right)^2 \ln\Lambda / (m_z v_{Ti} v_{Tz})^2 \qquad \text{with} \quad \ln\Lambda = \text{Coulomb-logarithm}$$

we arrive at the effective friction coefficient

$$\beta^* = \frac{2 m_z v_{Tz}}{m_i v_{Ti}^2}\,\frac{c_s}{\pi R_o} + \frac{3 m_i m_z v_{Ti} v_{Tz}}{8\sqrt{\pi} Z n_p \ln\Lambda}\left(\frac{\frac{c_s}{\pi R_o}}{\frac{e^2}{4\pi\varepsilon_o}}\right)^2 \tag{A4}$$

neglecting the ζ - dependence of the temperatures.

Appendix B

In the limit $\Delta^2 \varkappa_I \to \infty$ corresponding to the boundary condition $\bar{a}(+\infty, p) = 0$ the solution eqs.(2o a,b) simplify to the following form, if $F(\varrho, p) = 0$ for $\varrho > \Delta$

for $-\infty \leq \varrho \leq 0$ (plasma core, $q_{II} = \sqrt{p + \varkappa_{II}}$)

$$\bar{a}_{II}(\varrho, p) = \int_{-\infty}^{0} d\sigma\, F(\sigma, p) \left[\frac{\exp\left(-q_{II}|\varrho - \sigma|\right)}{2q_{II}} + \frac{\exp\left(-q_{II}|\varrho + \sigma|\right)}{2q_{II}} \left(\frac{q_{II} - q_I}{q_{II} + q_I} \right) \right] +$$

$$+ \int_{0}^{\Delta} d\sigma\, F(\sigma, p) \frac{\exp\left(-q_{II}|\varrho| - q_I \sigma\right)}{q_{II} + q_I} \qquad (B1)$$

and for $0 \leq \varrho \leq \Delta$ (scrape-off layer, $q_I = \sqrt{p + \varkappa_I}$)

$$\bar{a}_I(\varrho, p) = \int_{0}^{\Delta} d\sigma\, F(\sigma, p) \left[\frac{\exp\left(-q_I|\varrho - \sigma|\right)}{2q_I} + \frac{\exp\left(-q_I|\varrho + \sigma|\right)}{2q_I} \left(\frac{q_I - q_{II}}{q_I + q_{II}} \right) \right] +$$

$$+ \int_{-\infty}^{0} d\sigma\, F(\sigma, p) \frac{\exp\left(-q_I \varrho - q_{II}|\sigma|\right)}{q_I + q_{II}} \qquad (B2)$$

Whereas the inverse Laplace transform of the terms in brackets poses no problem when applying the standard formulae from ref.[5] and the convolution theorem, i.e.

$$L^{-1}\left(\frac{\exp(-q_R x)}{2q_R}\right) = \frac{\exp(-\varkappa_R D_\perp t)}{2\sqrt{\pi D_\perp}}\ \frac{\exp\left(-\dfrac{x^2}{4D_\perp t}\right)}{\sqrt{t}} \tag{B3}$$

and

$$L^{-1}\left(\frac{\exp(-q_R x)}{2q_R}\ \frac{q_R - q_S}{q_R + q_S}\right) = \frac{\exp(-\varkappa_R D_\perp t)}{2\sqrt{\pi D_\perp}}\int_0^t \frac{d\tau}{\tau\sqrt{t-\tau}}\exp\left(-\frac{x^2}{4D_\perp(t-\tau)} + (\varkappa_R - \varkappa_S)D_\perp\frac{\tau}{2}\right) I_1\left((\varkappa_R - \varkappa_S)D_\perp\frac{\tau}{2}\right) \tag{B4}$$

which are valid for $x \geq 0$, the transformation of the residual terms in eqs.(B1) and (B2) deserves some attention.

In order to avoid mathematical complications, we treat the inverse Laplace transform of the residual terms separately for $\varrho = 0$ and $|\varrho| > 0$. By careful application of the tables of ref.[5,6] we find

$$L^{-1}\left(\frac{1}{q_R + q_S}\right) = \frac{\exp(-\varkappa_S D_\perp t)}{2\sqrt{\pi}\ \sqrt{D_\perp t}^{\,3}}\ \frac{1-\exp\left(-(\varkappa_R - \varkappa_S)D_\perp t\right)}{\varkappa_R - \varkappa_S} \tag{B5}$$

$$L^{-1}\left(\exp(-q_S|\sigma|)\right) = \begin{cases} \dfrac{|\sigma|}{2\sqrt{\pi}\ \sqrt{D_\perp t}^{\,3}}\exp\left(-\varkappa_S D_\perp t - \dfrac{\sigma^2}{4D_\perp t}\right) & \text{for } |\sigma| > 0 \\[2ex] \dfrac{2\delta(t)}{D_\perp} & \text{for } \sigma = 0 \end{cases} \tag{B6}$$

and

$$L^{-1}\left(q_S \exp(-q_S|\sigma|)\right) = -\frac{\exp\left(-\varkappa_S D_\perp t - \frac{\sigma^2}{4D_\perp t}\right)}{2\sqrt{\pi}\sqrt{D_\perp t}^3}\left(1-\frac{\sigma^2}{2D_\perp t}\right) + \frac{4}{D_\perp}\,\delta(\sigma)\,\delta(t)$$

$$\text{with} \quad \lim_{t\to 0} \frac{\exp\left(-\varkappa_S D_\perp t - \frac{\sigma^2}{4D_\perp t}\right)}{2\sqrt{\pi D_\perp t}} = \delta(\sigma) \qquad \text{(B7)}$$

By application of the convolution theorem we obtain from eqs.(B5) to (B7):

for $\underline{\varrho = 0}$

$$L^{-1}\left(\frac{\exp(-q_S|\sigma|)}{q_R+q_S}\right) = \frac{\exp(-\varkappa_S D_\perp t)}{4\pi(\varkappa_R-\varkappa_S)D_\perp^2}\int_0^t d\tau \; \frac{1-\exp\left(-(\varkappa_R-\varkappa_S)D_\perp\tau\right)}{\sqrt{\tau\,(t-\tau)}^3}\,|\sigma|\,\exp\left(-\frac{\sigma^2}{4D_\perp(t-\tau)}\right) \qquad \text{(B8)}$$

and for $\underline{|\varrho|>0}$

$$L^{-1}\left(\frac{\exp(-q_R|\varrho|-q_S|\sigma|)}{q_R+q_S}\right) = L^{-1}\left(\frac{q_R-q_S}{\varkappa_R-\varkappa_S}\exp(-q_R|\varrho|-q_S|\sigma|)\right) = \frac{\int_0^t d\tau\, G(\tau)}{(\varkappa_R-\varkappa_S)D_\perp} \qquad \text{(B9)}$$

$$G(\tau) = \left[4\delta(\tau)\delta(\sigma) - \frac{\left(1-\frac{\sigma^2}{2D_\perp\tau}\right)}{2\sqrt{\pi D_\perp}} \frac{\exp\left(-\varkappa_S D_\perp \tau - \frac{\sigma^2}{4D_\perp\tau}\right)}{\sqrt{\tau}^3} \right] \frac{|\varrho|}{2\sqrt{\pi D_\perp}} \frac{\exp\left(-\varkappa_R D_\perp(t-\tau) - \frac{\varrho^2}{4D_\perp(t-\tau)}\right)}{\sqrt{t-\tau}^3} +$$

$$+ \frac{|\sigma|}{2\sqrt{\pi D_\perp}} \frac{\exp\left(-\varkappa_S D_\perp \tau - \frac{\sigma^2}{4D_\perp\tau}\right)}{\sqrt{\tau}^3} \frac{\left(1-\frac{\varrho^2}{2D_\perp(t-\tau)}\right)}{2\sqrt{\pi D_\perp}} \frac{\exp\left(-\varkappa_R D_\perp(t-\tau) - \frac{\varrho^2}{4D_\perp(t-\tau)}\right)}{\sqrt{t-\tau}^3}$$

By rearranging terms and performing the integration over $\delta(\tau)$ the formula for $|\varrho| > 0$ can be transformed into the expression

$$L^{-1}\left(\frac{\exp(-q_R|\varrho|-q_S|\sigma|)}{q_R+q_S}\right) = \frac{|\varrho|}{\sqrt{\pi}\,(\varkappa_S-\varkappa_R)\sqrt{D_\perp}^3} \frac{\exp\left(-\varkappa_R D_\perp t - \frac{\varrho^2}{4D_\perp t}\right)}{\sqrt{t}^3}\,\delta(\sigma) +$$

$$(B10)$$

$$+ \frac{\exp(-\varkappa_R D_\perp t)}{4\pi(\varkappa_S-\varkappa_R)D_\perp^2} \int_0^t \frac{d\tau}{\sqrt{\tau(t-\tau)}^3} \exp\left(-(\varkappa_S-\varkappa_R)D_\perp\tau - \frac{\varrho^2}{4D_\perp(t-\tau)} - \frac{\sigma^2}{4D_\perp\tau}\right)\left(-|\varrho|+|\sigma|+\frac{|\varrho\sigma|}{2D_\perp}\left(-\frac{|\varrho|}{t-\tau}+\frac{|\sigma|}{\tau}\right)\right)$$

which together with eqs.(B3), (B4) and (B8) is used in the solution, eqs.(22 a,b).

Appendix C

In order to guarantee continuity of the function $A_o^o(\varrho, t)$ at the separatrix $\varrho = 0$ we must be shure that

in the range $0 \leq \sigma \leq \Delta$

$$\frac{1}{2\sqrt{\pi}\,\varkappa^*\sqrt{D_\perp^3}} \int_0^{\tau'} d\tau \, \frac{\exp(\varkappa^* D_\perp \tau) - 1}{\sqrt{\tau(\tau'-\tau)}^{\,3}} \; \sigma \exp\left(-\frac{\sigma^2}{4D_\perp(\tau'-\tau)}\right) = \tag{C1}$$

$$\frac{\exp\left(-\frac{\sigma^2}{4D_\perp \tau'}\right)}{\sqrt{\tau'}} + \int_0^{\tau'} \frac{d\tau}{\tau} \, \frac{\exp\left(-\frac{\sigma^2}{4D_\perp(\tau'-\tau)} + \varkappa^* D_\perp \frac{\tau}{2}\right)}{\sqrt{\tau'-\tau}} I_1\left(\varkappa^* D_\perp \frac{\tau}{2}\right)$$

and in the range $-\infty \leq \sigma \leq 0$

$$\frac{1}{2\sqrt{\pi}\,\varkappa^*\sqrt{D_\perp^3}} \int_0^{\tau'} d\tau \, \frac{\exp(-\varkappa^* D_\perp \tau) - 1}{\sqrt{\tau(\tau'-\tau)}^{\,3}} \; \sigma \exp\left(-\frac{\sigma^2}{4D_\perp(\tau'-\tau)}\right) = \tag{C2}$$

$$\frac{\exp\left(-\frac{\sigma^2}{4D_\perp \tau'}\right)}{\sqrt{\tau'}} - \int_0^{\tau'} \frac{d\tau}{\tau} \, \frac{\exp\left(-\frac{\sigma^2}{4D_\perp(\tau'-\tau)} - \varkappa^* D_\perp \frac{\tau}{2}\right)}{\sqrt{\tau'-\tau}} I_1\left(\varkappa^* D_\perp \frac{\tau}{2}\right)$$

Since eq.(C2) results from eq.(C1) by substituting $\sigma \to -\sigma$ and $\varkappa^* \to -\varkappa^*$, it suffices to prove eq.(C1). For this purpose we start with writing the lhs. of eq.(C1) in the form

$$\frac{1}{\varkappa^*\sqrt{\pi D_\perp}} \frac{\partial}{\partial \sigma} \int_0^{\tau'} d\tau \, \frac{1 - \exp(\varkappa^* D_\perp \tau)}{\sqrt{\tau}^{\,3}} \, \frac{\exp\left(-\frac{\sigma^2}{4D_\perp(\tau'-\tau)}\right)}{\sqrt{\tau'-\tau}} \tag{C3}$$

Due to its origin the integral is of convolution type and can therefore be transformed into

$$\frac{2}{\varkappa^*}\sqrt{\frac{\pi}{D_\perp}}\,\frac{\partial}{\partial\sigma}\;L^{-1}\left(\left(\sqrt{p-\varkappa^* D_\perp}-\sqrt{p}\right)\frac{\exp\left(-\frac{\sigma}{\sqrt{D_\perp}}\sqrt{p}\right)}{\sqrt{p}}\right) \tag{C4}$$

since

$$\left.\begin{aligned} &L\left(\frac{1-\exp(\varkappa^* D_\perp \tau)}{\sqrt{\tau}^{3}}\right) = 2\sqrt{\pi}\left(\sqrt{p-\varkappa^* D_\perp}-\sqrt{p}\right) \\ &\text{and} \\ &L\left(\frac{\exp\left(-\frac{\sigma^2}{4D_\perp\tau}\right)}{\sqrt{\tau}}\right) = \sqrt{\frac{\pi}{p}}\;\exp\left(-\frac{\sigma}{\sqrt{D_\perp}}\sqrt{p}\right) \end{aligned}\right\} \tag{C5}$$

where L and L^{-1} denote respectively the direct and the inverse Laplace transform. Performing the σ-differentiation in the argument of the inverse Laplace transform we have

$$-\frac{2\sqrt{\pi}}{\varkappa^* D_\perp}\;L^{-1}\left(p\left(\sqrt{\frac{p-\varkappa^* D_\perp}{p}}-1\right)\frac{\exp\left(-\frac{\sigma}{\sqrt{D_\perp}}\sqrt{p}\right)}{\sqrt{p}}\right) \tag{C6}$$

From the tables of the inverse Laplace transform (p.17o and 246 of ref.[5] and p.781 of ref.[6]) we obtain

$$\int_0^{\tau'} d\tau \left[2\,\delta(\tau) + \frac{d}{d\tau}\left(\exp\left(\varkappa^* D_\perp \frac{\tau}{2}\right)\left(I_o\left(\varkappa^* D_\perp \frac{\tau}{2}\right) - I_1\left(\varkappa^* D_\perp \frac{\tau}{2}\right)\right)\right)\right]\frac{\exp\left(-\frac{\sigma^2}{4D_\perp(\tau'-\tau)}\right)}{\sqrt{\tau'-\tau}}$$

where the τ - differentiation yields $\qquad \exp\left(\varkappa^* D_\perp \frac{\tau}{2}\right)\,\dfrac{I_1\left(\varkappa^* D_\perp \frac{\tau}{2}\right)}{\tau}$ (C7)

I_o and I_1 are modified Bessel functions of zero resp. first order. Thus, by rearranging terms and performing the integration over the Delta-function, we finally arrive at the rhs. of eq.(C1).

Appendix D

In the limit $\Delta^2\varkappa_I \to \infty$ we obtain from eq.(21), if $F(\varrho,p) = 0$ for $\varrho > \Delta$

$$\bar{\gamma}^*(p) = \int_{-\infty}^{0} d\sigma\, F(\sigma,p)\, \frac{q_I \exp(-q_{II}|\sigma|)}{q_I + q_{II}} - \int_{0}^{\Delta} d\sigma\, F(\sigma,p)\, \frac{q_{II}\exp(-q_I\sigma)}{q_I + q_{II}} \qquad \text{(D1)}$$

Using eq.(B6) and performing the inverse Laplace transformation (in analogy to the formulae following eq.(C4))

$$L^{-1}\left(\frac{q_R}{q_R + q_S}\right) = -\frac{\exp(-\varkappa_R D_\perp t)}{\varkappa_R - \varkappa_S} L^{-1}\left(p\left[\sqrt{\frac{p-(\varkappa_R-\varkappa_S)}{p}} - 1\right]\right)$$

$$= \frac{\exp(-\varkappa_R D_\perp t)}{2D_\perp}\left(2\delta(t) + \frac{d}{dt}\left[\exp\left((\varkappa_R-\varkappa_S)D_\perp\frac{t}{2}\right)\left[I_0\left((\varkappa_R-\varkappa_S)D_\perp\frac{t}{2}\right) - I_1\left((\varkappa_R-\varkappa_S)D_\perp\frac{t}{2}\right)\right]\right]\right) \qquad \text{(D2)}$$

where the t-differentiation yields $\exp\left((\varkappa_R-\varkappa_S)D_\perp\frac{t}{2}\right) \dfrac{I_1\left((\varkappa_R-\varkappa_S)D_\perp\frac{t}{2}\right)}{t}$

we get by application of the convolution theorem

$$L^{-1}\left(\frac{q_R\exp(-q_S|\sigma|)}{q_R + q_S}\right) = \int_0^t d\tau\, \frac{\exp(-\varkappa_R D_\perp\tau)}{2D_\perp}\left[2\delta(\tau) + \right. \qquad \text{(D3)}$$

$$\left. + \exp\left((\varkappa_R-\varkappa_S)D_\perp\frac{\tau}{2}\right)\frac{I_1\left((\varkappa_R-\varkappa_S)D_\perp\frac{\tau}{2}\right)}{\tau}\right] \frac{|\sigma|}{2\sqrt{\pi D_\perp}} \frac{\exp\left(-\varkappa_S D_\perp(t-\tau) - \frac{\sigma^2}{4D_\perp(t-\tau)}\right)}{\sqrt{t-\tau}^{\,3}}$$

and finally arrive at the formula

$$L^{-1}\left(\frac{q_R \exp(-q_S|\sigma|)}{q_R + q_S}\right) = \tag{D4}$$

$$= \frac{|\sigma| \exp(-\varkappa_S D_\perp t)}{4\sqrt{\pi}\sqrt{D_\perp}^3}\left[\frac{\exp\left(-\frac{\sigma^2}{4D_\perp t}\right)}{\sqrt{t}^3} + \int_0^t \frac{d\tau}{\sqrt{t-\tau}^3} \exp\left(-\frac{\sigma^2}{4D_\perp(t-\tau)} - (\varkappa_R - \varkappa_S)D_\perp\frac{\tau}{2}\right)\frac{I_1\left((\varkappa_R-\varkappa_S)D_\perp\frac{\tau}{2}\right)}{\tau}\right]$$

which is used in the formulation of eq.(24).